FINNISH METEOROLOGICAL INSTITUTE
CONTRIBUTIONS

NO. 49

INVERSE PROBLEMS IN STELLAR OCCULTATION

VIKTORIA SOFIEVA

Department of Engineering Physics and Mathematics
Institute of Mathematics
Helsinki University of Technology

Dissertation for the degree of Doctor of Philosophy to be presented with due permission of the Department of Engineering Physics and Mathematics for public examination and debate in Auditorium E at Helsinki University of Technology (Espoo, Finland) on the 22nd of April, 2005, at 12 noon.

Finnish Meteorological Institute
Helsinki, 2005

ISBN 951-697-610-7 (paperback)
ISBN 951-22-7597-X (pdf)
ISSN 0782-6117

Yliopistopaino
Helsinki, 2005

FINNISH METEOROLOGICAL INSTITUTE

Published by Finnish Meteorological Institute
Vuorikatu 24, P.O. Box 503
FIN-00101 Helsinki, Finland

Series title, number and report code of publication
Contributions 49, FMI-CONT-49

Date
March 2005

Authors
Viktoria Sofieva

Name of project

Commissioned by

Title

Inverse problems in stellar occultation

Abstract

Remote sensing plays a key role in monitoring the atmosphere, which becomes increasingly important for the Earth's changing environment. The stellar occultation technique is a novel method to monitor vertical distribution of ozone and other trace gases from the troposphere to the upper mesosphere. GOMOS (Global Ozone Monitoring by Occultation of Stars) flying on board the European Space Agency's ENVISAT satellite is the first operational stellar occultation instrument.

Satellite measurements are indirect, and therefore inversion methods play a key role in the retrieval of atmospheric parameters. This dissertation is dedicated to inversion methods for stellar occultation measurements and to the optimization of retrievals.

Optimization of retrievals by inclusion of a priori information about smoothness of atmospheric profiles is considered. Two methods are developed. One of them –"the target resolution method"– develops the classical Tikhonov regularization. The second method includes smoothness a priori information in the form of Bayesian optimal estimation. The methodology for creating a priori information about smoothness of atmospheric profiles is developed.

This dissertation considers optimal selection of measurements based on information theory, aiming at optimal design of future instruments, as well as at improved efficiency of the current data processing. Two optimization problems, both taking the information content of the measurements as a criterion, are defined and discussed. The selecting procedures were developed, compared with each other and existing methodologies and applied to selection of the most informative channels for GOMOS measurements in the UV-Visible wavelength range.

The dissertation presents a feasibility study for retrieval of temperature and density profiles from pointing measurements by stellar occultation instruments. This study introduces extra geophysical parameters that can be obtained from GOMOS measurements.

The inversion methods developed are applied to GOMOS measurements. However, the methods are formulated in a general form that allows their application beyond the GOMOS mission.

Publishing unit
Finnish Meteorological Institute, Earth Observation Unit

Classification (UDC)
517.9, 519.72,
551.501.793, 551.507.362.2,
551.508.95, 551.510

Keywords
inverse problems, atmospheric remote sensing, occultation of stars, GOMOS, ozone, information theory

ISSN and series title
0782-6117 Finnish Meteorological Institute Contributions

ISBN
951-697-610-7 (paperback), 951-22-7597-X (pdf)

Language
English

Pages
110

Sold by
Finnish Meteorological Institute / Library
P.O.Box 503, FIN-00101 Helsinki
Finland

Note

Price

Acknowledgements

The work presented in this dissertation has been carried out in the Aeronomy group of the Finnish Meteorological Institute during the years 2000–2005.

I hearty thank Dr. Erkki Kyrölä, the head of the Aeronomy group, my supervisor and my co-author in many papers, who gave me the opportunity to work at FMI and who introduced me into the "GOMOS world". He has been always open for all kinds of scientific discussions. It has been a pleasure to work under his guidance.

I want to express my gratitude to Prof. Erkki Somersalo, my supervisor at Helsinki University of Technology, for very valuable advices related to inverse problems and smoothly-going guidance.

I warmly thank Dr. Johanna Tamminen, my colleague at Aeronomy group, my co-author in many papers and my current chief, for interesting discussions, helpful criticism and for her comprehensive support.

I also wish to thank my referees, Prof. Jari Kaipio and Dr. Didier Fussen for their positive criticism and very valuable comments on this work.

I thank my co-authors Prof. Heikki Haario, Prof. Esko Kyrö, Prof. Markku Lehtinen for interesting ideas and enlightening discussions.

It is my pleasure to thank Prof. Risto Pellinen, Prof. Tuija Pulkkinen, Prof. Jarkko Koskinen, Prof. Yrjö Viisanen and Prof. Petteri Taalas for providing excellent working conditions.

Existence of the GOMOS instrument was vital for this work. I am thankful to all the people who have worked in the GOMOS project for years, whose enthusiasm and huge work made the GOMOS mission possible. I thank all members of GOMOS CAL/VAL team from Service d'Aeronomie (France), IASB (Belgium), ACRI (France), ESTEC (Netherlands) and ESRIN (Italy) and colleagues from A.M. Oboukhov Institute of Atmospheric Physics (Russia) for interesting discussions related to GOMOS.

I am grateful to Prof. Gottfried Kirchengast (University of Graz, Austria) for valuable comments related to temperature profiling.

I thank the Arctic Research Center team of the Finnish Meteorological Institute for providing ozone sounding data.

I thank Prof. Gilbert Leppelmeier for his support and help with the English. I wish to thank my nearest colleagues in the Aeronomy group, Seppo Hassinen, Pekka Verronen and Annika Seppälä for pleasant working atmosphere and interesting discussions. I thank Seppo also for helping me with computers.

I am thankful to my family and relatives for encouragement during this work, especially to my children Alexey and Svetlana for their patience and to my husband Mikhail for his all-round support.

This work has been financially supported by European Space Agency and the Academy of Finland. The Magnus Ehrnrooth fund and the Vilho, Yrjö and Kalle Väisälä fund have sponsored my participation in IGARSS-2003 and COSPAR-2004 symposia, respectively.

Helsinki, March 2005

Viktoria Sofieva

Contents

List of original publications

I V. F. Sofieva, J. Tamminen, H. Haario, E. Kyrölä and M. Lehtinen: Ozone profile smoothness as a priori information in the inversion of limb measurements, *Annales Geophysicae*, 2004, Vol. 22, No. 10, pp. 3411–3420

II V. F. Sofieva, E. Kyrö, E. Kyrölä: Smoothness of ozone profiles: analysis of 11-years of ozone sonde measurements at Sodankylä, *Annales Geophysicae*, 2004, Vol. 22, No. 8, pp. 2723–2727

III V. F. Sofieva and E. Kyrölä: Information approach to optimal selection of the spectral channels, *Journal of Geophysical Research*, 108(D16), 4513, doi: 10.1029/2002JD002980, 2003

IV V. F. Sofieva and E. Kyrölä: Abel integral inversion in occultation measurements, in Occultations for Probing Atmosphere and Climate, edited by G. Kirchengast, U. Foelshe and A. Steiner, Springer Verlag, 2004, pp. 77– 86

V V. F. Sofieva, E. Kyrölä, J. Tamminen and M. Ferraguto: Atmospheric density, pressure and temperature profile reconstruction from refractive angle measurements in stellar occultation, in Occultations for Probing Atmosphere and Climate, edited by G. Kirchengast, U. Foelshe and A. Steiner, Springer Verlag, 2004, pp. 289–298

VI V. F. Sofieva, E. Kyrölä, M. Ferraguto and GOMOS CAL/VAL team: From pointing measurements in stellar occultation to atmospheric temperature, pressure and density profiling: simulations and first GOMOS results, IGARSS 2003, ISBN: 0-7803-7930-6 IEEE

V. Sofieva is responsible for the major work in all six publications, as well as for the manuscripts writing.

1 Introduction

This dissertation is dedicated to inversion methods for stellar occultation measurements and to the optimization of retrievals. The work was motivated by problems that have been encountered in the data processing of measurements by the GOMOS (Global Ozone Monitoring by Occultation of Stars) instrument on board the Envisat satellite. The dissertation consists of three parts. The first part deals with optimization of retrievals by inclusion of a priori information about smoothness of constituents profiles in the atmosphere and with development of a methodology for creating this a priori information. The second part is dedicated to optimal selection of measurements based on information theory, aiming at optimal design of future instruments, as well as at improved efficiency of the data processing. The third part introduces extra geophysical parameters (air density, pressure and temperature), which can be obtained from the pointing measurements by stellar occultation instruments.

The inversion methods developed are applied to GOMOS measurements. However, the methods are formulated in a general form that allows their application beyond the GOMOS mission.

The dissertation consists of six original publications that will be referred to by roman numerals (I–VI). The major contributions of the individual papers are as follows. Publ.I discusses inclusion of a priori information about smoothness of atmospheric profiles in inversion algorithms. Two methods are developed. One of them – "the target resolution method"– develops the classical Tikhonov regularization. The second method includes a priori information about smoothness of atmospheric profiles in the form of Bayesian optimal estimation. In Publ.II, the methodology for creating a priori information about smoothness of atmospheric profiles is developed. In Publ.III, the methods for selection of measurement subsets using information theory are examined. Two optimization problems, both taking the information content of the measurements as a criterion, are defined and discussed. The selecting procedures were developed, compared with each other and existing methodologies and applied to selection of the most informative channels for GOMOS measurements in the UV-Visible wavelength range. In Publ.IV, it is shown that occultation geometry under a spherical symmetry assumption leads to models described by the Abel integral equations. Analyzing general properties of the Abel transform, this work derives practical rules for discretization and for solution of inverse problems containing Abel-type integral equations. Publ.V and Publ.VI present a feasibility study for retrieval of temperature and density profiles from pointing measurements by stellar occultation instruments. This study introduces extra geophysical parameters that can be obtained from the GOMOS measurements. Inclusion of a priori information is discussed and error analysis is performed.

The overview section is organized as follows: Chapters 2-4 are dedicated to the description of the forward model and inverse methods for the main GOMOS mission: monitoring of ozone and trace gases in the atmosphere. In particular, in Chapter 2, the occultation principle, the forward model and the inversion strategy are introduced. Chapter 3 summarizes the results of PUBL.I and PUBL.II. Chapter 4 is dedicated to the information theory approach for optimal selection of measurements (PUBL.III). Chapter 5 discusses refractive measurements by the GOMOS instrument and inverse problems for retrieval of geophysical parameters from these measurements (PUBL.V and PUBL.VI).

2 Stellar occultation and inverse problems

2.1 The changing atmosphere

Measurements of chemical composition of the atmosphere during the past 40 years have clearly demonstrated that the concentration of several key components exhibit systematic trends. Detection of the ozone hole, significant increase of greenhouse gas concentrations and global mean surface temperature are the warning signs of environmental change.

On March 1, 2002 ESA launched a large environmental satellite, Envisat, which provides measurements of the atmosphere, oceans, land and ice. Envisat carries ten scientific instruments, including three instruments dedicated to atmospheric composition sounding: MIPAS, SCIAMACHY and GOMOS. GOMOS is the acronym for Global Ozone Monitoring by Occultation of Stars. Its major objective is the monitoring of the global vertical distribution of ozone and other trace gases from the upper troposphere to the upper mesosphere.

Ozone is a minor constituent in the Earth's atmosphere but it plays a crucial role in shielding Earth's biosphere against solar UV-radiation. Ozone is a central element in stratospheric chemistry and it has an important role in maintaining the thermal structure of the stratosphere. The heat released by the dissociation of ozone drives the stratospheric circulation that distributes ozone from the ozone production areas around the equator toward polar regions. Ozone is also one of the main greenhouse gases.

Observations in the mid-1980's revealed a large springtime ozone hole over Antarctica and subsequent analyses have also shown a general slow declining trend of the total ozone content in the stratosphere. The key driving process behind the decline is the release of anthropogenic CFC gases to the atmosphere. After a long, slow transport to the stratosphere complex CFC molecules are dissociated by the solar ultraviolet radiation and chlorine atoms are released into the stratospheric air. Increased amounts of chlorine atoms amplify the normal catalytic destruction cycles of ozone. In addition to this ('normal') homogeneous chemistry, the heterogeneous chemistry on polar stratospheric clouds or on surfaces of volcanic aerosol particles lead to a faster loss of ozone. This explains the severe loss of ozone over Antarctica together with the low temperatures developed during the stable winter vortex over the South Pole. International treaties, starting from the Montreal Protocol of 1988, have limited the amount of CFC gases released to the atmosphere, causing reduction of their quantities in the troposphere. Due to very long drift times to the stratosphere these positive trends will affect the stratospheric chlorine concentrations slowly: the estimated recovery time for the ozone loss is about 50 years.

Adequate ozone content in the atmosphere is necessary for the normal functioning of the biosphere and therefore we need to monitor systematically the

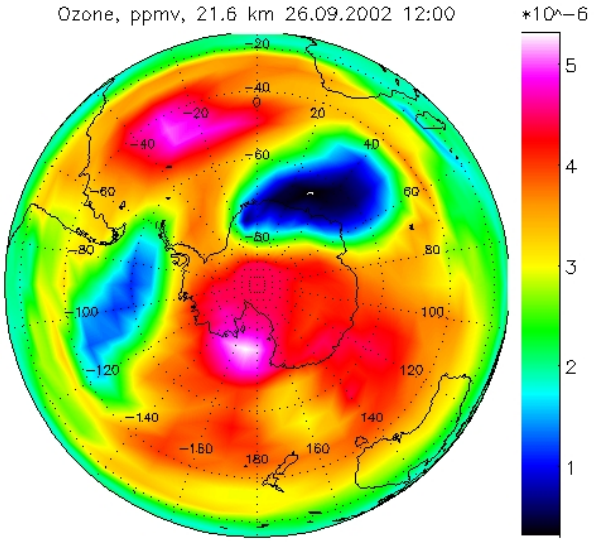

Figure 2.1. Split of the ozone hole into two holes in September 2002. Assimilated GOMOS and OSIRIS data. Courtesy of Seppo Hassinen, FMI.

global distribution of ozone. Even after the very intensive research in the past 20 years, some questions in the ozone problem remain unresolved. Perhaps the most important one is the coupling of the greenhouse effect and the ozone problem. The enhanced greenhouse effect cools the stratosphere and therefore slows down chemical reactions but also creates opportunities for buildup of stratospheric clouds needed in the heterogeneous chemistry. Dynamics can also play a significant role in shaping ozone distribution. For example, the ozone hole over the Antarctica was split in September 2002 (Figure 2.1). It is assumed that the split was generated by planetary wave activity.

One of the main purposes of Envisat is to provide measurement data on the Earth's changing atmosphere. The GOMOS mission aims to answer the following questions:

- What is the vertical distribution and the trend of ozone in the stratosphere and in the mesosphere over all the world?
- What is the effect of the limitation on CFC release?
- Are the chemistry and dynamics of ozone well understood, i.e. do model predictions agree with measurements?

These objectives require long-term measurements of ozone and other trace gases with high accuracy, global coverage and good vertical resolution.

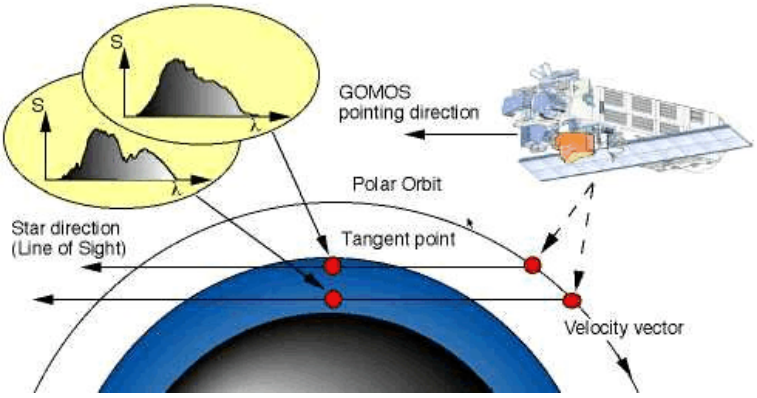

Figure 2.2. Occultation principle [http://envisat.esa.int/dataproducts/gomos].

Satellite measurements are indirect, and therefore inversion methods play a key role in the retrieval of atmospheric profiles. The scientific objectives of the GOMOS mission require accurate and efficient inversion algorithms. Specific features of inverse problems from satellite measurements can be outlined as follows:

1. The retrieved products should be as accurate as possible. The error estimates should be correct.

2. The vertical resolution should be sufficient to resolve the dynamical structures and peak values of concentrations.

3. The inversion procedure should be numerically efficient due to vast amount of data.

2.2 UV-Visible spectral measurements by GOMOS

GOMOS is the first operational stellar occultation instrument. However, first occultation measurements were made already 30 years ago [Hays and Roble, 1968; Roble and Hays, 1972]. The solar occultation technique [Chu et al., 1989] had a key role in deriving ozone trends in 1979-2000. Recently, the UVISI instrument on the MSX satellite has carried successfuly steller occultaions in 1996-2001 deriving ozone concentrations in the stratosphere [Yee et al., 2002; DeMajistre and Yee, 2002; Vervack et al., 2002].

The benefit of the occultation principle is its self-calibrating measurement concept (for references and reviews of occultation method, see [Hays and Roble, 1968; Elliot, 1979; Smith and Hunten, 1990; Korpela, 1991; Kyrölä et al., 1993; Bertaux et al., 2004; Kyrölä et al., 2004]). The reference stellar spectrum is first measured when a star can be seen above the atmosphere. During the occultation, the measurements through the atmosphere provide spectra modified by absorption, scattering and refraction (Figure 2.2). When these occulted spectra $S(\lambda, h)$

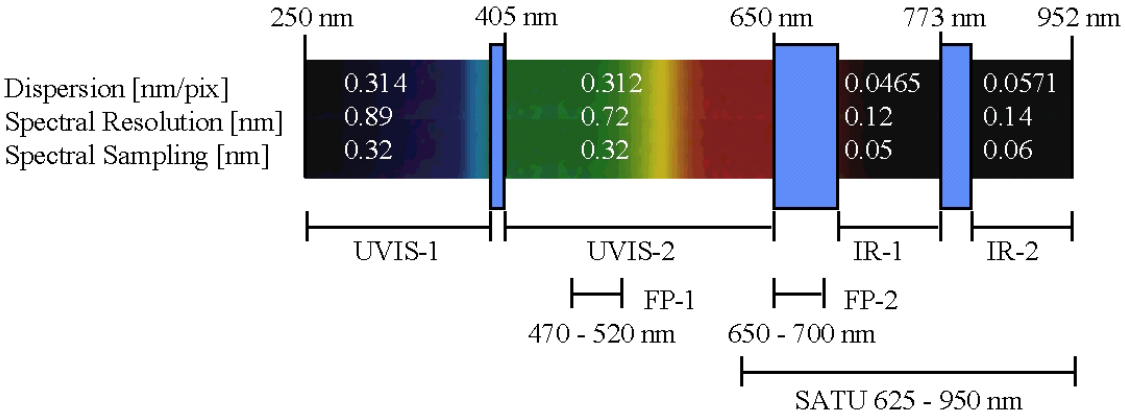

Figure 2.3. Spectral coverage and resolution of the GOMOS detectors [http://envisat.esa.int/dataproducts/gomos].

are divided by the reference spectrum $S_{\text{star}}(\lambda)$, nearly calibration-free horizontal transmission spectra are obtained:

$$T(\lambda, h) = \frac{S(\lambda, h)}{S_{\text{star}}(\lambda)}. \tag{2.1}$$

Here λ and h denote wavelength and tangent altitude, respectively. These transmissions are the input data for retrieval of atmospheric constituent densities.

Since stars are point sources of quite low-intensity light, special instruments are needed for the recording of stellar spectra. The challenging pointing system consisting of a steering-front mechanism (SFM) and a star tracker (SATU) allows detection of a star and keeping the image of the star in the centre of the slit (which is incorporated in order to minimize the scattered solar light in bright limb occultations). GOMOS includes two spectrometers, one operating in the UV-Visible and the other at infrared wavelengths. The detectors are two-dimensional charge-coupled devices (CCD); they allow measurements of radiation coming from extended sources and from stars with good spectral resolution. Light from a point source is focused on the few central lines of the detector, while the diffuse light scattered from the atmosphere is spread over the CCD. Therefore, it is possible to estimate the scattering contribution to the total signal. The wavelength range of detectors and spectral resolution is shown in Figure 2.3.

Each UV-visible spectrum contains 1416 spectral values in the wavelength range 250-675 nm, and one stellar occultation comprises 70-100 spectra at different tangent altitudes in the range of ∼10-140 km. One complete stellar occultation thus contains over 100 000 data points. Vertical profiles of ozone, NO_2, NO_3, aerosol and air density are retrieved from the UV-Visible spectrometer measurements. The next section presents the formal description of the forward model.

2.2.1 Forward model

The stellar light and the background signal (scattered light) are recorded by CCD. The background signal is negligible in dark limb occultations. In this dissertation, only dark limb measurements are considered.

The signal $S_{\text{obs}}(\lambda, t)$ recorded by each pixel of the CCD (marked by the wavelength λ) at the moment t can be presented as a sum of a useful signal $S_{\text{att}}(\lambda, t)$ and noise $S_{\text{noise}}(\lambda, t)$

$$S_{\text{obs}}(\lambda, t) = S_{\text{att}}(\lambda, t) + S_{\text{noise}}(\lambda, t). \tag{2.2}$$

The noise term in (2.2) contains the dark current of the CCD, photon noise and readout noise. Statistics of photocounts obeys a Poisson distribution, which can be approximated to good accuracy by a normal distribution due to large variance values. The readout noise is assumed to have a normal distribution. The mean dark current can be estimated and subtracted from the detected signal as an offset signal.

The noiseless signal $S_{\text{att}}(\lambda, t)$ originates from the occulted star and can be represented as

$$S_{\text{att}}(\lambda, t) = \int W_{\text{ins}}(\lambda, \lambda', t) T_{\text{atm}}(\lambda', t) S_{star}(\lambda') d\lambda', \tag{2.3}$$

where $W_{\text{ins}}(\lambda, \lambda', t)$ represents an instrumental transmission function, $S_{\text{star}}(\lambda)$ is a non-attenuated stellar spectrum and $T_{\text{atm}}(\lambda, t)$ is an atmospheric transmission function. When the stellar spectrum is measured above the atmosphere, the reference spectrum is obtained

$$S^{\text{star}}_{\text{obs}}(\lambda, t) = \int W_{\text{ins}}(\lambda, \lambda', t) S_{\text{star}}(\lambda') d\lambda' + S_{\text{noise}}(\lambda, t). \tag{2.4}$$

The atmospheric transmission function $T_{\text{atm}}(\lambda, t)$ has a complicated structure. First, it contains the component due to absorption and scattering (extinction) of gases, which can be modelled by using the well-known Lambert-Beer law

$$T_{\text{ext}} = e^{-\tau}, \tag{2.5}$$

where the optical depth τ is given by

$$\tau(\lambda) = \sum_j \int \sigma_j(\lambda, \mathrm{T}(\bar{r}(s))) \rho_j(\bar{r}(s)) ds. \tag{2.6}$$

Here the ρ_j's are constituent densities depending on the position $\bar{r}$ and the σ_j's are the temperature-dependent absorption or scattering cross sections. The integration is performed along the optical path joining the instrument and the source. The cross sections and typical transmission functions are shown in Figures 2.4 and 2.5, respectively.

Second, the atmospheric transmission function $T_{\text{atm}}(\lambda, t)$ contains also a component generated by refractive effects. These effects are:

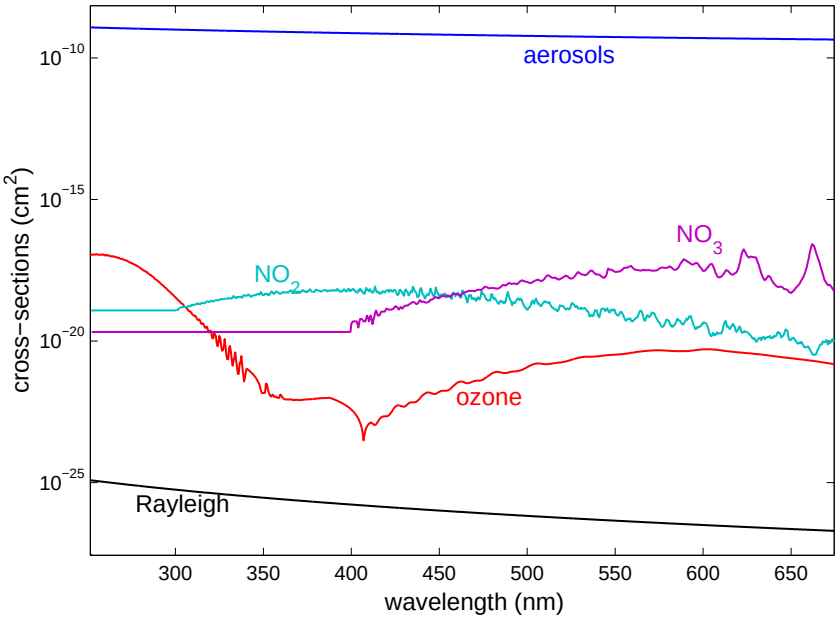

Figure 2.4. The absorption and scattering cross sections in the UV-Visible wavelength range.

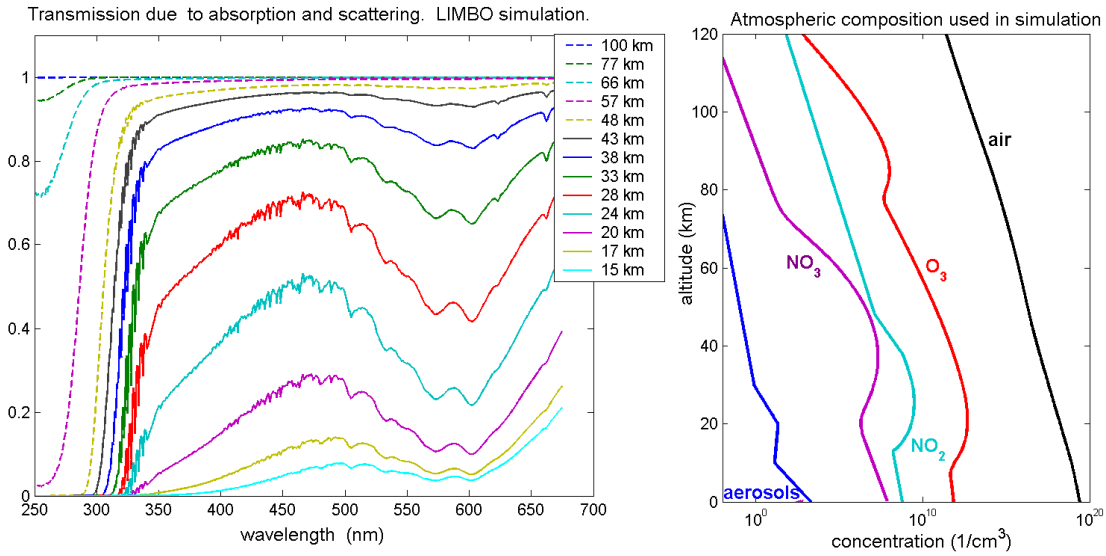

Figure 2.5. Left: transmission including the effects of absorption and scattering at selected altitudes simulated with LIMBO [Kyrölä et al., 1999]; right: atmospheric composition used in the simulation.

- Refraction.

  A nearly exponential decrease of the atmospheric air density leads to bending of rays coming from a star. The bending angle increases with decreasing altitude.

- Refractive dilution.

  The change of the propagation direction in the atmosphere will result to dilution of the related intensity.

- Chromatic aberration.

  The dependence of the refractive index of the atmosphere on wavelength leads to a spatial separation of rays of different colors.

- Scintillation.

  This results from diffraction of light passing through air density irregularities. If the stellar light is measured with a high-frequency device, the measured intensity exhibits fluctuations that may exceed its regular value by several hundred percent.

The refractive effects are discussed in more detail in Chapter 5. The most elaborate analysis of refractive effects and scintillation can be found in [Dalaudier et al., 2001; Kan et al., 2001; Gurvich and Brekhovskikh, 2001; Gurvich and Chunchuzov, 2003].

The influence of absorption and refractive effects on received light at satellite level is quite different: refraction changes the direction of propagation but has no effect on the energy (number of photons) transported by light, while absorption removes photons (and thus energy) from a light beam but does not change its direction. It is assumed that the absorption and refraction affect the atmospheric transmission independently, so it can be expressed as a product [GOMOS ESL, 1999]

$$T_{\mathrm{atm}}(\lambda, t) = T_{\mathrm{ext}}(\lambda, t) T_{\mathrm{ref}}(\lambda, t). \tag{2.7}$$

The finite measurement time $\Delta t = 0.5$ s of GOMOS should be also taken into account. By combining (2.2), (2.3), (2.5), (2.6) and (2.7), we get the forward model of the GOMOS measurements:

$$\begin{aligned} S_{\mathrm{obs}}(\lambda, t) = \frac{1}{\Delta t} \int_{\Delta t} \int W_{\mathrm{ins}}(\lambda, \lambda', t') T_{\mathrm{refr}}(\lambda', t') T_{\mathrm{scint}}(\lambda', t') \times \\ \exp\left(- \sum_j \int \sigma_j(\lambda', \mathrm{T}(s)) \rho_j(s) ds \right) S_{\mathrm{star}}(\lambda') d\lambda' dt' + S_{\mathrm{noise}}(t). \end{aligned} \tag{2.8}$$

The typical geometry scales of GOMOS measurements are shown in Figure 2.6.

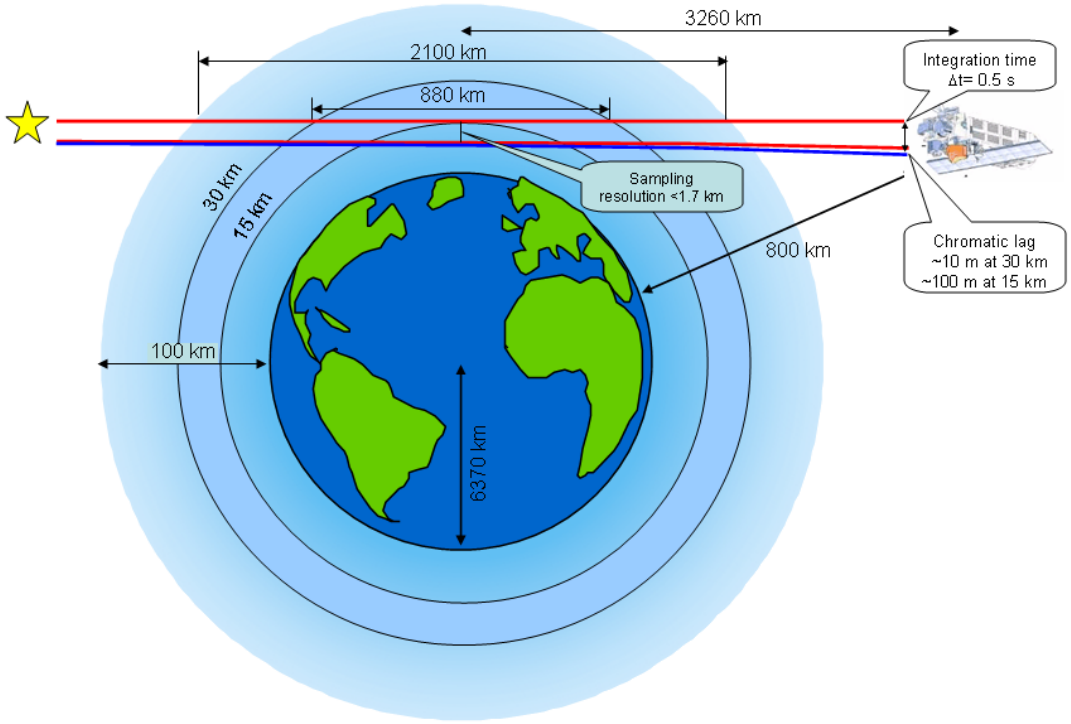

Figure 2.6. GOMOS geometry scales. The altitude of the satellite orbit is 800 km. Taking atmosphere thickness 100 km, the longest distance that a light ray travels in the atmosphere is ∼2100 km (at a tangent altitude of 15 km). The distance between the two points at which this ray intersects the 30 km altitude level is ∼880 km. The measurement time $\Delta t = 0.5$ s defines the sampling vertical resolution, which is better than 1.7 km. The chromatic separation of rays both at satellite level and in the atmosphere (not shown) is significantly smaller than the sampling resolution: it is ∼10 m at 30 km altitude for rays of wavelengths 500 nm and 675 nm.

2.2.2 GOMOS retrieval strategy

The GOMOS processing starts with various instrumental corrections. First, the mean dark current is subtracted from the reference and attenuated spectra. Second, the reference star spectrum is averaged from sufficiently many measurements above the atmosphere, thus giving an accurate estimate of the star spectrum S_{star}. Then the spectrum observed through the atmosphere is divided by the reference spectrum, yielding the atmospheric transmission function:

$$T_{\text{atm}} = \frac{S_{\text{obs}}}{S_{\text{star}}}. \tag{2.9}$$

The component due to refractive effects is estimated and removed from the transmission data (GOMOS ESL [1999, 1998]; Dalaudier et al. [2001])

$$T_{\text{ext}}^{\text{obs}} = \frac{T_{\text{atm}}}{T_{\text{ref}}}. \tag{2.10}$$

The refractive term T_{ref} is presented in the form

$$T_{\text{ref}} = T_{\text{d}} T_{\text{scin}}, \tag{2.11}$$

where the component T_{d} corresponding to regular refractive effects (refractive dilution) is modulated by the scintillation component T_{scin}. The dilution term T_{d} can be estimated from ray tracing calculations. In the GOMOS processing, ECMWF air density data are used in ray tracing.

For scintillation correction, GOMOS is equipped with two fast photometers sampling simultaneously stellar flux in low-absorption wavelength regions ($\sim$495 nm and $\sim$ 675 nm) at a frequency of 1 kHz. The estimation of T_{scin} consists of detecting fluctuations from the scintillation measurements and averaging them over the 0.5 s integration time of spectrometers. This estimation assumes that all high-frequency fluctuations in the photometer signal (except for noise) are due to scintillations, while fluctuations due to structure in the vertical profiles of absorbing constituents affect only the low-frequency component of the signal. Another hypothesis of the GOMOS refractive effects correction is that light rays of different colors come through exactly the same refractive structures, so that the signal perturbations at different wavelengths are identical after appropriate shifting and stretching as a result of the regular refractive effect. The second hypothesis is always satisfied in vertical occultations (in orbital plane), but may be violated in oblique occultations if isotropic turbulence is well developed. Validity of these assumptions is discussed in more detail in [Dalaudier et al., 2001; Kyrölä et al., 2005].

After the correction of refractive effects, the transmission spectra, which are approximately described by equations (2.5) and (2.6) are obtained. These transmission spectra provide the basis for retrieval of atmospheric constituent densities.

It is possible, in principle, to discretize the atmosphere into volume cells and perform a kind of atmospheric tomography (global inversion). However, the dimension of the problem makes this approach unfeasible: 1500 spectrally resolved data at approximately 80 altitudes give 120 000 measurement points in one occultation; GOMOS makes 300-500 occultations every 24 hours; 10 unknown concentrations in at least 8000 volume cells (80 divisions in altitude $\times$ 20 latitudinal divisions $\times$ 5 longitudinal divisions) give 80 000 parameters to fit. Furthermore, the temporal resolution would be lost with this approach.

Therefore, individual occultations are considered in the GOMOS processing. Three basic inversion schemes that evaluate individual occultations have been considered. All assume local spherical symmetry of the atmosphere. In the first

scheme, transmission data from every tangent height are inverted to horizontal column densities for different constituents (spectral inversion). For every constituent, the collection of horizontal column densities at successive tangent heights is converted to vertical density profiles (vertical inversion). The second scheme first calculates the vertical profile of the wavelength-dependent extinction. Then the vertical profiles of constituents can be reconstructed from the vertical profiles of extinction using the cross sections. The third method starts from the transmissions from all tangent heights and inverts the constituent densities in one step [Sihvola, 1994; Haario et al., 2004; Vanhellemont et al., 2004]. The different approaches to inversion of GOMOS data are schematically shown also in Figure 2.7.

The present GOMOS processing scheme relies on the first method, i.e. spectral inversion followed by vertical inversion. This method has been chosen for two reasons. The first is a significant reduction in amount of data that must be handled at a time. The 'spectral first' approach contributes to the fast reduction in size of data. The second reason is related to the observation geometry of GOMOS. The result of the spectral inversion – horizontal column densities – might be also useful for assimilation of GOMOS measurements into atmospheric models. The current GOMOS processing scheme allows various applications of GOMOS data (Figure 2.7).

The split of the inversion into the spectral inversion and the vertical inversion is mathematically correct only if the cross-section kernel in (2.6) is independent of the spatial variables, otherwise we need to use so-called effective cross-section method [Sihvola, 1994]. In this method, the optical depth τ is presented in the form

$$\tau(\lambda, \ell) = \sum_j \int \rho_j(z(s))\sigma_j(\lambda, \mathrm{T}(z(s)))ds = \sum_j \sigma_j^{\mathrm{eff}}(\lambda, \ell)N_j, \tag{2.12}$$

where N_j is the line density of the species j

$$N_j = \int_\ell \rho_j(z(s))ds \tag{2.13}$$

and

$$\sigma_j^{\mathrm{eff}}(\lambda, \ell) = \frac{\int_\ell \sigma_j(\lambda, \mathrm{T}(z(s)))\rho_j(z(s))ds}{N_j} \tag{2.14}$$

is the effective cross section of species j.

The use of the effective cross sections allows the separation of the inversion problem into two parts. The spectral inversion part is given by (2.12) with the horizontal column densities N_j as unknowns. The vertical inversion part is given by (2.13) with local density $\rho_j(z)$ as the unknowns. The two parts are, however, coupled together by the unknown effective cross sections. In order to take into account the coupling effect, the processing makes use of an iterative loop over spectral and vertical inversions.

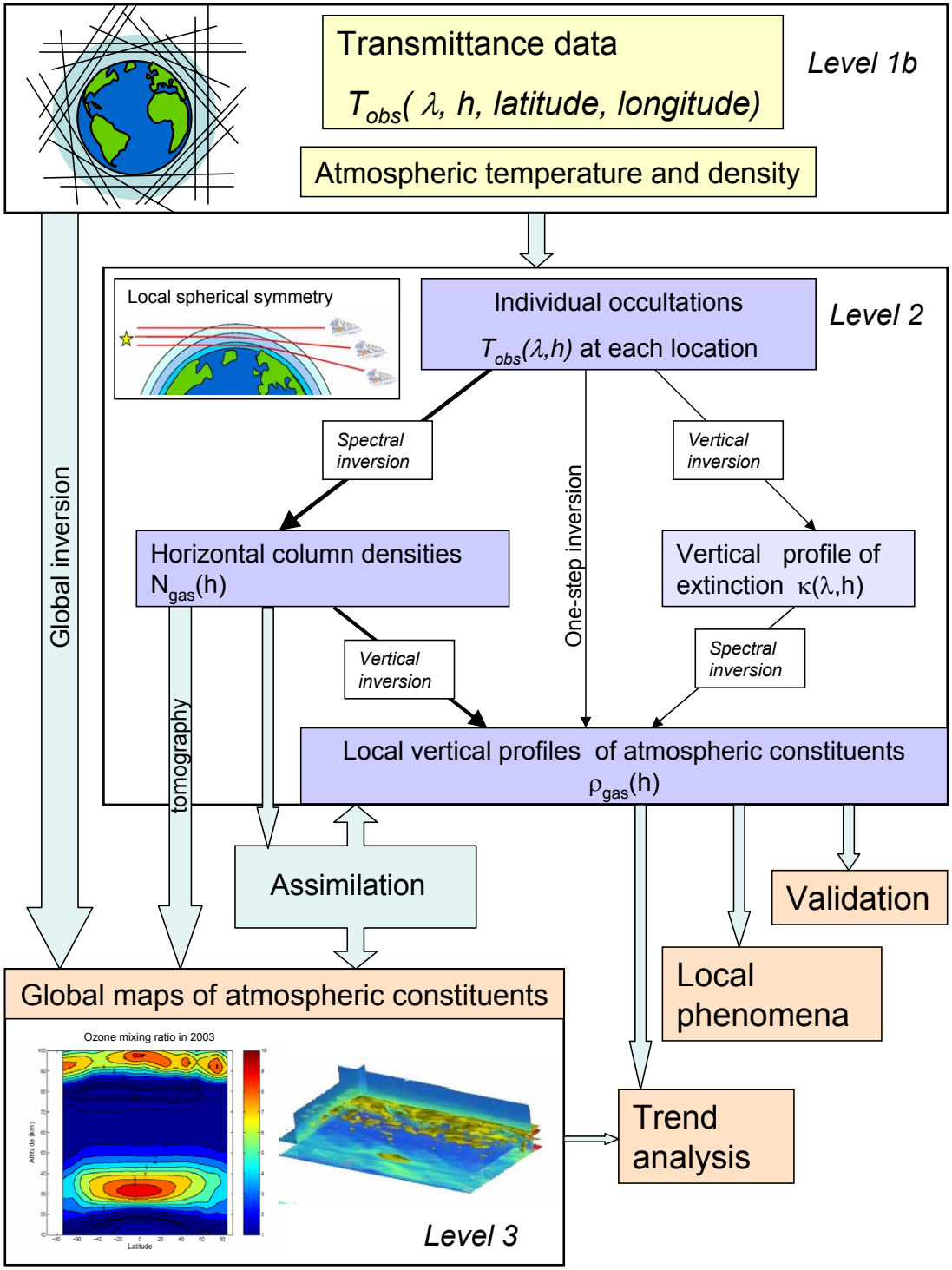

Figure 2.7. Different approaches to inversion and possible applications of GOMOS data.

2.2.3 Spectral inversion

The spectral inversion problem is that of determination of horizontal column densities from the observed transmission data T_{obs}. It is coupled with the vertical inversion via an iterative loop that uses the effective cross sections. At each loop, the problem can be written as

$$\mathbf{T}_{\text{obs}} = \exp(-\mathbf{\Sigma N}) + \boldsymbol{\varepsilon}, \tag{2.15}$$

where $\mathbf{T}_{\text{obs}}$ is a vector of observed transmittances that include absorption and scattering, $\mathbf{\Sigma}$ is a matrix of cross sections and $\mathbf{N}$ is a vector of unknown horizontal column densities.

The estimations of horizontal column densities is based on the standard maximum likelihood method (more complete but also computationally more expensive methods are discussed in [Tamminen and Kyrölä, 2001; Tamminen, 2004]). Under the assumption of a Gaussian distribution of the measurement noise, it is equivalent to minimization of the χ^2 statistics

$$\chi^2 = (\mathbf{T}_{\text{mod}}(\mathbf{N}) - \mathbf{T}_{\text{obs}})^T \mathbf{C}^{-1} (\mathbf{T}_{\text{mod}}(\mathbf{N}) - \mathbf{T}_{\text{obs}}), \tag{2.16}$$

where $\mathbf{T}_{\text{mod}}$ is the modelled transmission and $\mathbf{C}$ is the covariance matrix of the transmission errors. The minimization is performed using the Levenberg-Marquardt algorithm [Press et al., 1992]. The covariance matrix $\mathbf{C}$ of the transmission errors has two components. The first (and dominating) $\mathbf{C}_{\text{obs}}$ is due to noise in measurements. If there is no operation destroying stochastic independence of errors, this covariance matrix is diagonal. In addition to measurement noise, the covariance matrix can also include the component $\mathbf{C}_{\text{mod}}$, which comes from various approximations and modelling errors. If the data statistics and the modelling error are Gaussian, the total error is a sum of these two:

$$\mathbf{C} = \mathbf{C}_{\text{obs}} + \mathbf{C}_{\text{mod}}. \tag{2.17}$$

The modelling errors are briefly discussed in [Kyrölä et al., 1993] and in PUBL.III; a more detailed analysis is presented in [Sofieva et al., 2005]. Specification of all modelling errors is a complicated task, and it is not yet fully solved.

The forward model can be linearized by simply taking logarithm of (2.15), so that at each altitude we have the standard linear model with additive noise

$$\boldsymbol{\tau} = -\ln \mathbf{T}_{\text{obs}} = \mathbf{\Sigma N} + \boldsymbol{\varepsilon}_1, \tag{2.18}$$

where $\boldsymbol{\tau}$ is a measurements vector (optical depth), and $\boldsymbol{\varepsilon}_1$ is a noise vector. The linearized form is convenient for the error analysis and sensitivity studies. However, the linearization is possible only if data are pre-processed in order to eliminate non-positive values. Furthermore, the linearization modifies the distribution of

the measurement noise, but provided $|\varepsilon_1| = \left|\frac{\varepsilon}{T_{\rm obs}}\right| \ll 1$ and $T_{\rm obs} > 0$ the Gaussian approximation still holds [Kyrölä et al., 1993; Tamminen and Kyrölä, 2001].

A specific aspect of the spectral inversion is discussed in PUBL.III, namely, the information content of measurements. It is defined by the structure of the forward model matrix $\mathbf{\Sigma}$, by the noise level and a priori information used in the inversion. The information approach is discussed also in Chapter 4 of this dissertation.

2.2.4 Vertical inversion

The vertical inversion aims to determine a vertical profile, $\rho(z)$, that fulfils the equation

$$N(z) = \int \rho(z(s))ds, \tag{2.19}$$

where N is any of the horizontal column densities inverted in the spectral inversion (2.15) and the integration is performed along the ray path. Assuming spherical symmetry of the atmosphere and ignoring refraction of rays, the vertical inversion problem (2.19) can be presented as an Abel integral equation

$$N(p) = 2\int_p^\infty \frac{\rho(r)rdr}{\sqrt{r^2 - p^2}}. \tag{2.20}$$

Here p is the ray perigee altitude. Vertical inversion consists of reconstruction of the vertical density profile $\rho(r)$ from the horizontal column densities $N(p)$, known for different values of the impact parameter. The formal solution can be written as

$$\rho(r) = -\frac{1}{\pi}\int_r^\infty \frac{N'(p)dp}{\sqrt{p^2 - r^2}}. \tag{2.21}$$

The vertical inversion problem in its continuous formulation (2.20) is ill-posed; this follows from the compactness of the forward model operator. This is discussed in PUBL.IV.

In practice, we have only a finite number of measurements. The problem of reconstruction of a continuous function from a finite number of measurements is inherently ill-posed. However, a discrete representation obtained by dividing the atmosphere into layers according to a measurement structure and making certain assumptions about the profile behavior within the layers (constant, linear, polynomial altitude dependence) transform the problem to an even-determined problem. In GOMOS processing, the number of layers is chosen equal to the number of measurements (horizontal column densities). Different discretization schemes of the vertical inversion (2.20) are discussed in PUBL.IV. It is found that the collocation method [Gorenflo and Vessella, 1991] gives the most numerically efficient and stable pole-free discretization.

In the collocation approach, it is first assumed that the upper limit in the integral (2.20) is finite (R). Suppose that there are M measurements at the points $x_1, x_2, ..., x_M$: $N_i = N(x_i)$. We generate the layers structure $r_i, i = 1, ..., M+1$ so that $x_i \in (r_i, r_i + 1)$ (usually it is chosen $x_i = (1-s)r_i + s\, r_{i+1}$, where s is the shift between the layers and the measurements structures). For the midpoint collocation method, $\rho(r)$ is replaced by $\tilde{\rho}(r) = \rho(x_i)$ when $r_i < r \leq r_{i+1}$, for the trapezoidal collocation method $\rho(r)$ is replaced by a linear interpolation term $\rho(r) = \frac{(r_{j-1}-r)\rho(r_j)+(r-r_j)\rho_{j-1}}{r_{j-1}-r_j}$ and for polynomial collocation method by a polynomial interpolation term. Then Eq.(2.20) is collocated at the points x_i by the formula

$$2\int_{x_i}^{R} \frac{\rho(r)rdr}{\sqrt{r^2-p^2}} = N_i \qquad \text{for } i = 1, 2, ..., M. \tag{2.22}$$

Finally, we arrive at the triangular linear system $K_{ij}\rho_j = N_i$, $i = 1, 2, ..., M$. Let us note that the weak singularity disappears as the result of integration

$$\int_{x_i}^{r_i} \frac{a_0 + a_1 r + ... + a_m r^m}{\sqrt{r^2 - x^2}} dr$$

in calculation of the elements K_{ii} of the matrix $\mathbf{K}$. In GOMOS-related literature, the midpoint collocation discretization is often called the 'onion peeling' method.

Regardless of the discretization, the vertical inversion in the matrix form can be written as

$$\mathbf{N} = \mathbf{K}\boldsymbol{\rho} + \boldsymbol{\varepsilon}, \tag{2.23}$$

where $\mathbf{K}$ is the forward model (kernel) matrix, $\mathbf{N}$ is a vector of measurements (horizontal column densities), $\boldsymbol{\rho}$ is a vector of unknowns (profile) and $\boldsymbol{\varepsilon}$ is a vector of measurement noise. In GOMOS processing, bending of ray trajectories due to refraction is also taken into account. The discretized GOMOS vertical inversion problem (3.4) is well-conditioned (the condition number of the forward model matrix $\mathbf{K}$ for a typical occultation is ~ 25), so it can be solved with usual matrix inversion. The inversion is slightly noise-amplifying by a factor $\sim$2 (PUBL.IV). However, in the case of dim stars, the reconstructed profiles are significantly contaminated with noise.

2.3 Characterization of retrieved profiles

The most complete characterization of the reconstructed profiles would be given by their posterior distribution. However, the posterior distribution often is not retrieved. In practice, the error of reconstruction is assumed to have Gaussian distribution; it is characterized by its covariance matrix.

Let us consider the forward model (2.23). Given the retrieved profile $\hat{\boldsymbol{\rho}}$ in the form of $\hat{\boldsymbol{\rho}} = \mathbf{GN}$, where $\mathbf{G}$ is the inversion matrix, the total error (i.e. a deviation of a retrieved profile $\hat{\boldsymbol{\rho}}$ from the true one $\boldsymbol{\rho}$) is

$$\hat{\boldsymbol{\rho}} - \boldsymbol{\rho} = (\mathbf{GK} - \mathbf{I})\boldsymbol{\rho} + \mathbf{G}\boldsymbol{\varepsilon} = (\mathbf{A} - \mathbf{I})\boldsymbol{\rho} + \mathbf{G}\boldsymbol{\varepsilon}. \tag{2.24}$$

Here $\mathbf{A} = \mathbf{GK}$ is the matrix of averaging kernels, $\mathbf{I}$ is the unit matrix. The latter term in (2.24) is the error due to noise in measurements, while the former term describes the smoothing error caused by deviation of averaging kernels from delta-functions. The covariance of the total error (2.24) is [Rodgers, 2000]

$$\mathbf{C}_{\text{tot}} = (\mathbf{A} - \mathbf{I})\mathbf{C}_{\mathbf{e}}(\mathbf{A} - \mathbf{I})^T + \mathbf{G}\mathbf{C}_{\boldsymbol{\varepsilon}}\mathbf{G}^T, \tag{2.25}$$

where $\mathbf{C}_{\boldsymbol{\varepsilon}}$ is the covariance matrix of measurement noise and $\mathbf{C}_{\mathbf{e}}$ is the covariance of an ensemble of real profiles about the mean profile.

The concept of an averaging kernel allows further simplification in characterizing quality of profile retrievals. More generally, the averaging kernel can be defined as [Backus and Gilbert, 1970; Rodgers, 1990]:

$$A = \frac{\partial \widehat{\rho}}{\partial \rho}, \tag{2.26}$$

where $\widehat{\rho}$ is the retrieved profile and ρ is the true profile. The width of the averaging kernel can be used as a measure of resolution. One commonly used measure is the Backus-Gilbert spread $s(z)$ (e.g. Rodgers [2000]):

$$s(z) = 12 \int (z - z')^2 A^2(z, z') dz' / (\int A(z, z') dz')^2. \tag{2.27}$$

Another measure of resolution – a modified Backus-Gilbert spread – is briefly discussed in Publ.IV. The resolution and the error estimates are often used for simplified characterization of accuracy of retrieved profiles.

The GOMOS instrument is capable of retrieving the atmospheric profiles with a very good resolution. The averaging kernels of the pre-launch GOMOS inversion are sharply peaked (Publ.I, Figure 1). For a typical occultation, the resolution (Backus-Gilbert spread) is $\sim$2 km in the mesosphere and upper stratosphere, and is less than 1 km in the lower stratosphere and troposphere.

2.4 Specific features of stellar occultation measurements

The GOMOS measurements have specific features that are not typical for other remote sensing measurements.

The GOMOS instrument uses stars as a source of radiation. The stellar spectra strongly depend on visual magnitude and effective temperature of the star, and so does the signal-to-noise ratio. Values of signal-to-noise ratio for some types of star are shown in Figure 2.4.

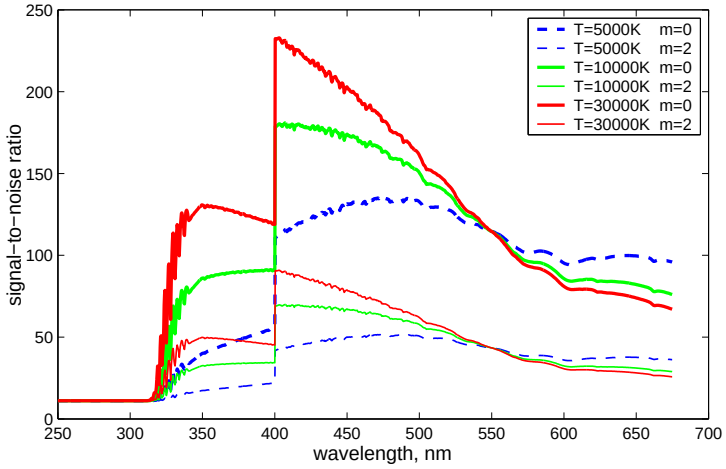

Figure 2.8. Signal-to-noise ratio for some stellar classes (simulation) at 30 km; visual magnitudes m and effective temperatures T are specified in the legend. The discontinuity around 400 nm is due to the spectral gap between two spectrometers.

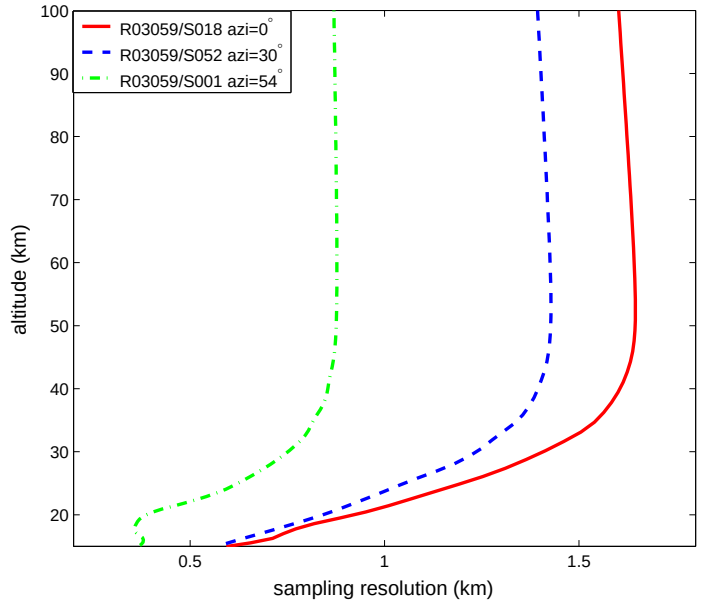

Figure 2.9. Sampling resolution in vertical (R03059/S018, azimuth=0°), typical (R03059/S052, azimuth=30°) and oblique (R03059/S001, azimuth=54°) occultations.

The second specific feature is the dependence of sampling resolution on the line-of-sight azimuth angle. The sampling resolution for different line-of-sight azimuth angles is shown in Figure 2.4. For very oblique occultations it can be nearly twice as good as for vertical ones. The measurement grid becomes denser in the lower part of the atmosphere due to refraction. These two features are inherently determined by the design of the GOMOS instrument and measurement principle. There is, however, one more feature that is defined not by the instrument, but by insufficient knowledge of atmospheric processes. It was found that the error in reconstructed gas profiles depends not only on the stellar spectral class, but also on the obliqueness of occultation. This error is generated by incomplete scintillation correction: the current algorithm does not correct the isotropic part of the scintillation.

As a result of these specific features, GOMOS measurements are actually a collection of measurements that differ from each other in signal-to-noise ratio and vertical resolution. Global coverage for monitoring the atmosphere requires robustness of the inversion algorithm: it should give comparably good results also in cases of low signal-to-noise ratio. Publ.I considers regularization and inclusion of a priori information in the inversion aimed at this objective.

3 A priori information in inversion of stellar occultation measurements

The application of inversion methods that use a priori information to stellar occultation is discussed in Publ.I. Let us consider the linear forward model

$$\mathbf{y} = \mathbf{K}\mathbf{x} + \boldsymbol{\varepsilon}, \tag{3.1}$$

where $\mathbf{y}$ is the measurement vector, $\mathbf{K}$ is the forward model matrix, $\mathbf{x}$ is the state vector (a vector of unknown parameters) and $\boldsymbol{\varepsilon}$ is the vector of measurement noise. The essence of inclusion of a priori information is expressed by the Bayes' formula describing the posterior probability density function (*pdf*) $P(\mathbf{x}|\mathbf{y})$ via a likelihood function $P(\mathbf{y}|\mathbf{x})$ and a priori *pdf* $P_{\text{prior}}(\mathbf{x})$:

$$P(\mathbf{x}|\mathbf{y}) = \frac{P(\mathbf{y}|\mathbf{x})P_{\text{prior}}(\mathbf{x})}{P(\mathbf{y})}. \tag{3.2}$$

Here $P(\mathbf{y})$ a priori probability density of $\mathbf{y}$ characterizing a priori knowledge of the measurement data. This scaling factor $P(\mathbf{y})$ is often not needed in practice.

In many applications, the prior *pdf* is assumed to be Gaussian with a mean $\mathbf{x}_0$ and a covariance $\mathbf{C}_a$: $\mathbf{x}_a \sim \mathcal{N}(\mathbf{x}_0, \mathbf{C}_a)$. In this case, the maximum a posteriori (MAP) estimate of the retrieved profile $\mathbf{x}_{\text{MAP}}$ can be presented in the following form (e.g. Tarantola [1987])

$$\mathbf{x}_{\text{MAP}} = (\mathbf{K}^{\mathbf{T}}{\mathbf{C}_\varepsilon}^{-\mathbf{1}}\mathbf{K} + {\mathbf{C}_a}^{-\mathbf{1}})^{-\mathbf{1}}\mathbf{K}^{\mathbf{T}}{\mathbf{C}_\varepsilon}^{-\mathbf{1}}(\mathbf{y} - \mathbf{K}\mathbf{x_0}) + \mathbf{x_0}, \tag{3.3}$$

provided the measurement noise $\boldsymbol{\varepsilon}$ is also Gaussian: $\boldsymbol{\varepsilon} \sim \mathcal{N}(0, \mathbf{C}_\varepsilon)$ and mutually independent of the unknown $\mathbf{x}$.

3.1 Available a priori information. Methods for constructing a priori information

A priori information needed for application of (3.3) is not available with global coverage even for ozone. The climatological data [Fortuin and Kelder, 1998] can, in principle, be used as an a priori estimate of the mean of ozone profile, but the inter-annual variability of the climatology does not reflect that of individual profiles [Publ.I].

Nevertheless, in a few cases when an occultation is located near an ozone observation station, useful a priori information can be obtained. Publ.II develops the methodology for creation of 'smoothness a priori'. The smoothness of ozone profiles is characterized by the characteristic scale of the fine structure, which, in turn, is defined as the correlation length of the profile fluctuations. The analysis of the smoothness of ozone profiles based on 11-years ozone sonde measurements

at Sodankylä is performed. It is found that the characteristic scale has only slight seasonal variations and can therefore be considered as a relatively stable atmospheric characteristic.

For other trace gases, the smoothness of profiles can be used at the moment only as ad hoc guess. Analysis of all available data and their assimilation into dynamical and chemical transport models will allow obtaining useful a priori information in future.

3.1.1 The need for advanced data analysis

The signal-to-noise ratio in stellar occultation measurements strongly depends on stellar parameters (visual magnitude and effective temperature), and so does the error of the vertical profile reconstruction.

In pre-launch simulations significant non-physical oscillations of reconstructed ozone profiles for dim stars (visual magnitude >2.5) were observed but only for altitudes above 80 km and below 18 km (Publ.I, Fig.3). Therefore, no a priori information or regularization were explicitly used in the GOMOS baseline inversion, as the lowermost altitude of GOMOS measurements was expected to be ∼18 km.

GOMOS validation has shown that the noise level is slightly higher than expected. Additional errors come from incomplete scintillation correction. Analyses of GOMOS data have shown that a significant share of occultations (∼10%) is terminated at altitudes below 10 km. For especially bright stars, such as Sirius, GOMOS is able to follow the star even down to 5 km altitude. This enables GOMOS to probe also the troposphere, but advanced inversion methods are required because of the low signal-to-noise ratio in the troposphere.

The vertical resolution achieved in GOMOS measurements is better than the characteristic vertical scale of the ozone fine structures (1.0–1.4 km in the troposphere and in the lower stratosphere, according to Publ.II).

These features encourage application of regularization or including a priori information about profile smoothness in the GOMOS inversion. The inversion methods that use smoothness of atmospheric profiles are discussed in Publ.I.

3.2 Smoothness of atmospheric profiles as a priori information in retrievals

Publ.I discusses inclusion of a priori information about smoothness of atmospheric profiles in inversion algorithms. The smoothness requirement can be formulated in the form of Tikhonov-type regularization, where the smoothness of atmospheric profiles is considered as a constraint or in the form of Bayesian optimal estimation, where the smoothness of profiles can be included as a priori

information. Two retrieval methods are developed. One of them – Tikhonov-type regularization according to the target resolution – develops the classical Tikhonov regularization. The second method is the statistical optimization with smoothness a priori, which uses maximum a posteriori (MAP) estimates for retrieved profiles.

In this section, a short description of these methods is given. Following PUBL.I, we consider a linear forward model (which corresponds to GOMOS vertical inversion):

$$\mathbf{N} = \mathbf{K}\boldsymbol{\rho} + \boldsymbol{\varepsilon}, \tag{3.4}$$

where $\mathbf{N}$ is a vector of measurements (horizontal column densities), $\boldsymbol{\rho}$ is a vector of unknowns (profile values), and $\boldsymbol{\varepsilon}$ represents a vector of measurement noise.

3.2.1 Statistical optimization with smoothness a priori

In most cases a priori information includes only a general measure of smoothness of atmospheric profiles. Assuming that the neighboring discretized values of a retrieved profile cannot be too different, we can write

$$\rho_{i-1} + \rho_{i+1} - 2\rho_i = h_i^2 \varepsilon_i^{\mathrm{sm}}, \tag{3.5}$$

where $\varepsilon_i^{\mathrm{sm}}$ are mutually independent Gaussian random variables with the zero mean and h_i is the discretization grid. Alternatively, first order or higher order differences can be used in the left-hand side of (3.5). Explicit inclusion of the discretization step h_i allows definition of smoothness not depending on disretization grid. The equation (3.5) can be expressed in the matrix form as

$$\mathbf{H}\boldsymbol{\rho} = \boldsymbol{\varepsilon}^{\mathrm{sm}}, \tag{3.6}$$

where tri-diagonal matrix $\mathbf{H}$ approximates second derivatives:

$$\mathbf{H} = \mathrm{diag}\left[\frac{1}{h_i^2}\right] \begin{bmatrix} 0 & 0 & 0 & ... & 0 \\ 1 & -2 & 1 & ... & 0 \\ ... & .. & ... & ... & ... \\ 0 & ... & 1 & -2 & 1 \\ 0 & 0 & ... & 0 & 0 \end{bmatrix} \tag{3.7}$$

It corresponds to the prior distribution (smoothness a priori)

$$P_{\mathrm{prior}} \propto \exp(-\frac{1}{2}\boldsymbol{\rho}^T \mathbf{H}^T \mathbf{C}_{\mathrm{sm}}^{-1} \mathbf{H}\boldsymbol{\rho}), \tag{3.8}$$

where $\mathbf{C}_{\mathrm{sm}}$ is the covariance matrix of $\boldsymbol{\varepsilon}^{\mathrm{sm}}$. If the matrix $\mathbf{H}^T\mathbf{C}_{\mathrm{sm}}^{-1}\mathbf{H}$ is invertible, the prior distribution is Gaussian: $\boldsymbol{\rho}_a \sim \mathcal{N}(0, (\mathbf{H}^T\mathbf{C}_{\mathrm{sm}}^{-1}\mathbf{H})^{-1})$.

Provided $\boldsymbol{\rho}$ and $\boldsymbol{\varepsilon}$ are mutually independent random variables, the measurement noise $\boldsymbol{\varepsilon}$ is Gaussian: $\boldsymbol{\varepsilon} \sim \mathcal{N}(0, \mathbf{C}_\varepsilon)$, the a priori distribution is given by

(3.8) and Ker($\mathbf{K}$) $\cap$ Ker($\mathbf{H}$)=$\{0\}$, the MAP (maximum a posteriori) solution to the problem (3.4) is given by

$$\boldsymbol{\rho}_{\mathrm{sm}} = (\mathbf{K}^T\mathbf{C}_\varepsilon^{-1}\mathbf{K} + \mathbf{H}^T\mathbf{C}_{\mathrm{sm}}^{-1}\mathbf{H})^{-1}\mathbf{K}^T\mathbf{C}_\varepsilon{}^{-1}\mathbf{N}. \tag{3.9}$$

Indeed, under the assumptions made, the likelihood function is

$$P(\mathbf{N}|\boldsymbol{\rho}) \propto \exp\left(-\frac{1}{2}(\mathbf{N}-\mathbf{K}\boldsymbol{\rho})^T\mathbf{C}_\varepsilon^{-1}(\mathbf{N}-\mathbf{K}\boldsymbol{\rho})\right). \tag{3.10}$$

Substituting (3.10) and (3.8) into the Bayesian formula (3.2), we get a posteriori probability density function

$$\ln P(\boldsymbol{\rho}|\mathbf{N}) \propto -\frac{1}{2}\left((\mathbf{N}-\mathbf{K}\boldsymbol{\rho})^T\mathbf{C}_\varepsilon^{-1}(\mathbf{N}-\mathbf{K}\boldsymbol{\rho}) + \boldsymbol{\rho}^T\mathbf{H}^T\mathbf{C}_{\mathrm{sm}}^{-1}\mathbf{H}\boldsymbol{\rho}\right). \tag{3.11}$$

By differentiating (3.11) we get that the posterior *pdf* achieves its maximum when $\boldsymbol{\rho} = \boldsymbol{\rho}_{\mathrm{sm}}$, defined by (3.9). The condition Ker($\mathbf{K}$) $\cap$ Ker($\mathbf{H}$)=$\{0\}$ guarantees invertibility of the matrix $(\mathbf{K}^T\mathbf{C}_\varepsilon^{-1}\mathbf{K} + \mathbf{H}^T\mathbf{C}_{\mathrm{sm}}^{-1}\mathbf{H})$.

The solution $\boldsymbol{\rho}_{\mathrm{sm}}$ can also be computed without using the formula (3.9). Formulation of the equivalent least square problem for determination of $\boldsymbol{\rho}_{\mathrm{sm}}$ [Kaipio and Somersalo, 2005] allows its numerically efficient computation by methods of linear algebra.

The only information needed for application of this method are the uncertainties of the second differences $\mathbf{C}_{\mathrm{sm}}$, which can be obtained from analysis of high-resolution profile measurements such as ozone sonde data. The statistical optimization with smoothness a priori efficiently combines the measurements and a priori information, applying additional smoothing only when it is required by low signal-to-noise ratios.

3.2.2 Target resolution method

The classical Tikhonov regularized solution of the problem (3.4) can be derived as a minimizer of the functional

$$F(\lambda) = \|\mathbf{K}\boldsymbol{\rho} - \mathbf{N}\|^2 + \lambda\|\mathbf{H}\boldsymbol{\rho}\|^2. \tag{3.12}$$

Here λ is the regularization parameter and $\mathbf{H}$ is the matrix representing first, second (3.7) or higher order differences (which are assumed to be bounded, thus characterizing the smoothness of the solution), and $\|\cdot\|$ is ℓ_2-norm.

Provided that Ker($\mathbf{K}$)$\cap$Ker($\mathbf{H}$)=$\{0\}$, the Tikhonov-regularized solution of (3.12) exists, and it is unique. It is given by the formula

$$\hat{\boldsymbol{\rho}} = (\mathbf{K}^T\mathbf{K} + \lambda\mathbf{H}^T\mathbf{H})^{-1}\mathbf{K}^T\mathbf{N}. \tag{3.13}$$

The optimal choice of the regularization parameter λ is a central issue in the literature discussing the Tikhonov regularization. It can be chosen, for example,

according to the Morozov's discrepancy principle (e.g. Morozov [1993]; Hansen et al. [2000]), which states that λ should be chosen from the condition:

$$\|\mathbf{N} - \mathbf{K}\hat{\boldsymbol{\rho}}(\lambda)\| = \|\boldsymbol{\varepsilon}\|. \tag{3.14}$$

Application of the Tikhonov regularization as well as the statistical optimization with smoothness a priori discussed above leads to a certain degradation of resolution. The regularization parameter can be also chosen according to some target resolution, if the optimal value of the regularization parameter does not meet the resolution requirements. Then the actual vertical resolution does not depend on the instrumental noise and the discretization grid. This simplicity of profile characterization makes this method attractive. The details of its application are discussed in Publ.I.

Nowadays, it is the target resolution method that is used in the operational GOMOS inversion. The regularization parameters depending on altitude and on constituent are defined so that the actual vertical resolution (Backus-Gilbert spread) satisfies the resolution requirements.

3.2.3 Concluding remarks

Application of the two newly developed inversion methods – the target resolution method and the statistical optimization with smoothness a priori – to reconstruction of ozone profile from GOMOS measurements is discussed in Publ.I. Their efficiencies were compared with that of the original GOMOS inversion ('onion peeling') and the classical inversion methods (the standard Tikhonov regularization and the classical MAP estimate (3.3)). Realistic simulations for the typical measurement conditions with smoothness a priori information created from 10-years analysis of ozone sounding at Sodankylä and analysis of total retrieval error (including components due to measurement noise and due to smoothing properties of inversion) illustrate the advantages of the proposed methods. The following main conclusions can be drawn:

1. The standard Tikhonov regularization with smoothing parameter chosen according to the discrepancy principle is not recommended for the ozone profile retrieval from the GOMOS measurements, because the 'optimal' smoothing violates the resolution requirements: almost all fine structures of ozone profiles are smoothed out by this method.

2. The regularization with the choice of the smoothing parameters according to the resolution requirements is the most attractive method because of the predetermined vertical resolution, independence from measurement grid and from stellar properties. It is a kind of 'minimal guaranteed strategy', but it is not optimal in the statistical sense. The target resolution method is used in the operational GOMOS processing nowadays.

3. The statistical optimization with smoothness a priori efficiently combines measurement data and information on smoothness of profiles and gives the estimates with accuracy approaching that of the classical MAP estimates. It is a good alternative to the classical statistical optimization in cases when mean and/or standard deviation of retrieved quantities are not known.

4 Optimal selection of measurements: information theory approach

Remote sensing measurements of the atmosphere with high spectral resolution instruments provide a large amount of information about the atmosphere, but it is not evident how to use it efficiently. The number of measurements can significantly exceed the number of retrieved parameters. For example, the GOMOS UV-Visible spectrometers' sample at each altitude consists of approximately 1500 spectrally resolved data, while no more than 10 unknown parameters are retrieved. One of the commonly-used approaches for simplifying the retrieval is to select a smaller subset of data for analysis. The optimal selection of a measurement subset has two goals:

1) to reduce the dimension of a problem in order to speed up the data processing;

2) to detect the most informative measurements (in spectroscopy - spectral channels) with the aim of optimizing the design of future instruments.

The efficiency of measurements can be described by a wide range of parameters, such as the accuracy of the retrieved quantities, resolution and precision. For optimization problems, however, a single quantity, Figure of Merit, is required. C.D. Rodgers [1996] proposed characterizing the efficiency of measurements by their information content in the Shannon sense.

The information content of an experiment is a value that can be considered as the amount of knowledge obtained by making the experiment. It is defined as the reduction in the entropy of the probability density functions [Shannon and Weaver, 1949] before and after the experiment. The entropy of a continuous probability density function $P(x)$ is defined as

$$H(P) = -\int P(x)\log(P(x))dx, \tag{4.1}$$

where the integral is taken over the state space. For the Gaussian distribution with the covariance matrix $\mathbf{C}$ the entropy is determined by the formula

$$H(P) = \text{const} + \frac{1}{2}\ln|\mathbf{C}|, \tag{4.2}$$

where $|\mathbf{C}|$ is the determinant of $\mathbf{C}$. If the prior and posterior distributions are Gaussian, the information content I can be expressed as

$$I = \frac{1}{2}(\ln|\mathbf{C}_a| - \ln|\mathbf{C}|), \tag{4.3}$$

where $\mathbf{C}_a$ and $\mathbf{C}$ are the prior and posterior covariances, respectively.

The information content describes the reduction of the 'volume of uncertainty' caused by making an experiment, and generalizes the concept of signal-to-noise ratio in the state space [Rodgers, 2000]. Although the information content

is not the only Figure of Merit (e.g. Dudhia et al. [2002]), it is one of natural choices.

Consider the linear forward model, connecting a measurement vector $\mathbf{y}$ and a vector of unknowns $\mathbf{x}$:

$$\mathbf{y} = \mathbf{K}\mathbf{x} + \boldsymbol{\varepsilon}. \tag{4.4}$$

Here $\mathbf{K}$ is the forward model matrix and $\boldsymbol{\varepsilon}$ is a random error vector. The problem is assumed to be over-determined, i.e. a number of measurements significantly exceeds a number of unknowns.

Applying the statistical inversion to problem (4.4) (MAP estimate) and assuming that the noise $\boldsymbol{\varepsilon}$ and the retrieved vector $\mathbf{x}$ are mutually independent Gaussian random variables $\boldsymbol{\varepsilon} \sim \mathcal{N}(0, \mathbf{C}_\varepsilon)$, $\mathbf{x} \sim \mathcal{N}(\mathbf{x}_a, \mathbf{C}_a)$, we get the posterior covariance matrix $\mathbf{C}$ and the information content I in the form:

$$\mathbf{C}^{-1} = \mathbf{K}^T\mathbf{C}_\varepsilon^{-1}\mathbf{K} + \mathbf{C}_a^{-1} \tag{4.5}$$

$$I = \frac{1}{2}\ln|\mathbf{C}^{-1}\mathbf{C}_a| = \frac{1}{2}\ln|\mathbf{E} + \mathbf{K}^T\mathbf{C}_\varepsilon^{-1}\mathbf{K}\mathbf{C}_a|, \tag{4.6}$$

where $\mathbf{E}$ is a unit matrix.

Any removal of measurements (channels in spectroscopy) leads to a decrease in the information content (Publ.III). Consequently, the maximal information content corresponds to the initial over-determined problem. The problem of optimal subset selection consists of choosing such channels that contain 'almost all' of the original information content. Two formulations of the optimization problems with constraints, either limiting the number of measurements or the value of the information content are stated in Publ.III:

Optimization problem OP1 *Choose the minimal set of measurements providing the information content I_0, i.e.*

$$A = \min\{A_i \subseteq U \mid I_{A_i} \geq I_0\}, \tag{4.7}$$

where U is the set of channels and A_i are its subsets.

Optimization problem OP2 *Choose the subset of m channels from N available channels so that the information content is maximal, i.e*

$$I = \max_{A_i \subseteq U} I_{A_i}, \qquad \dim(A_i) = m. \tag{4.8}$$

Publ.III discusses the uniqueness of solution to these problems and the challenges in their solving. The problem of maximization of information content cannot be solved exactly either by integer programming methods, because of nonlinearity of the objective function, or with combinatorial methods, because of the astronomical number of different possible combinations of measurements. An effective procedure for searching for the optimal data subset is therefore needed. The sequential selection procedure proposed in [Rodgers, 1996] allows the choosing

of high-informative channel subsets. If there is no correlation between measurement errors, the information content can be computed efficiently. These ideas were applied to the AIRS sounder [Rodgers, 1996], the IASI instrument [Lerner et al., 2002] and the MIPAS instrument [Bennet et al., 1999; Dudhia et al., 2002].

In PUBL.III two new channel (measurement) selection procedures are proposed and developed: the sequential deselecting procedure and the fast algorithm for channel selection. These also provide approximations to solutions of the optimization problem. The efficiencies of these selection procedures and the sequential selection procedure of Rodgers [1996] are compared by means of a Monte Carlo generation of the forward model in a low-dimensional case. This statistical test has shown that the sequential deselecting procedure gives the best approximation to the global optimum of the problem. The numerical efficiency of each procedure is also discussed. As a conclusion, the application of the sequential deselecting procedure is recommended if numerical efficiency is not crucial.

As a real application, the selection of the most informative spectral channels for GOMOS measurements is considered in PUBL.III. Both the sequential selecting and deselecting procedures gave similar subsets of the most informative channels for ozone, NO_2, NO_3, air and aerosol retrieval. They cover most of the UV-visible wavelength range with a spectral gap at 370 - 400 nm. At each altitude, $\sim 50\%$ of the spectral channels are non-informative, and they can be removed from data processing without any significant reduction in performance. However, for different altitudes, different parts of the spectrum have high information content. As follows from PUBL.III (Figure 5), the UV part is very important for the upper atmosphere, while the visible channels become more significant for the lower atmosphere, where the UV part has negligible information content. From the point of view of instrument design it is therefore important to cover the whole UV-VIS spectrum, except for the wavelength band 370 - 400 nm: this has low information content for all altitudes.

For the GOMOS baseline inversion, the selection of the most informative channels is not so important, as the inversion is fast enough. However, channel selection can be an important consideration in alternative inversion algorithms, such as the one-step inversion.

5 Refractive measurements by GOMOS

Stellar occultation instruments must have a high pointing accuracy, because they follow point-like sources. These two features allow accurate measurements of the refractive angle in the limb viewing geometry. The determination of the stratospheric density and temperature profiles from the refractive-angle measurements by stellar occultation instruments is considered in Publ.V and Publ.VI. The refractive angles can be measured by GOMOS in two different ways. First, the refractive angles can be obtained from the recordings of the pointing system, which includes the steering front mechanism (SFM) and the star tracker (SATU). Second, the refractive angles can be retrieved with a high vertical resolution from bi-chromatic scintillation measurements using correlation analysis. Publ.V and Publ.VI discuss the first type of refractive angle measurements only.

The idea of reconstructing temperature profiles from measurements of refractive angle has a long history. The first feasibility studies were performed over 35 years ago [Tatarskiy, 1968a,b]. It was shown, that high-precision measurements of refractive angle (up to microradians) are required for accurate reconstruction of temperature. Development of radio-occultation technique has allowed accurate measurements of refractive angle. The radio occultation measurements are indirect: the refractive angle is reconstructed from the excess-phase data measured via Doppler-shift. Nowadays, the radio-occultation technique for temperature sounding of the troposphere and stratosphere has been investigated in depth [Kursinski et al., 1997; Steiner et al., 1999; Rieder and Kirchengast, 2001], and has been successfully validated [e.g., Kursinski et al. [1997]; Gorbunov and Kornblueh [2001]].

However, the possibility of stratospheric temperature profiling using refractive angle measurements by stellar occultation instruments has not been studied enough. The only attempt was made by the MSX-UVISI instrument [Vervack et al., 2002], but the accuracy of temperature reconstruction was rather poor. The pointing system of MSX-UVISI instrument is different from that one used in GOMOS.

Publ.V presents the feasibility study aimed at analysis of the accuracy achievable in temperature profiling with the GOMOS and COALA (a planned successor of GOMOS) instruments and at deriving the pointing accuracy requirements for the temperature profiling with accuracy of 1-2 K and the vertical resolution of 1-2 km. This study introduces extra geophysical parameters, which can be obtained from the GOMOS instrument.

5.1 Forward model

The forward model consists of the determination of the refraction angle from an assumed density profile in the atmosphere. We assume that the refractive index n

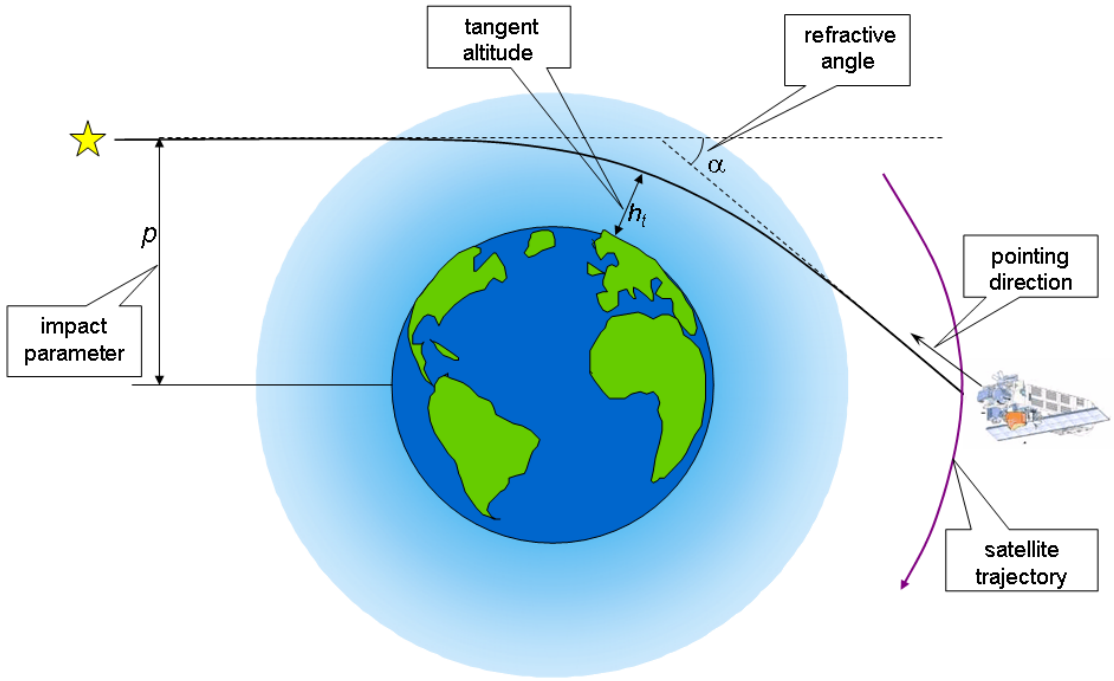

Figure 5.1. Refractive measurements by GOMOS: definition of parameters.

depends on the wavelength λ of the light and on the neutral air density ρ according to the Edlen formula [Edlen, 1966]:

$$n = 1 + C(\lambda)\frac{\rho}{\rho_0}, \tag{5.1}$$

where ρ_0 is the air density at the Earth's surface and $C(\lambda)$ is a constant depending on the wavelength λ as:

$$C(\lambda) = 10^{-6}\left(83.42 + \frac{24060}{130 - \lambda^{-2}} + \frac{160}{39 - \lambda^{-2}}\right), \tag{5.2}$$

where λ is in micrometers.

Under the spherical symmetry assumption, the refractive angle α may be determined as

$$\alpha(p) = -2p\int_{r_t}^{\infty}\frac{d(\ln n)}{dr}\frac{dr}{\sqrt{n^2r^2 - p^2}}, \tag{5.3}$$

where r_t is a tangent altitude and p is an impact parameter (for definitions of parameters, see Fig. 5.1).

Introduction of a new variable $y = nr$, which is often called a refractive

altitude, allows us to write (5.3) in the form of an Abel transform

$$\alpha(p) = -2p \int_p^\infty \frac{d(\ln n)}{dy} \frac{dy}{\sqrt{y^2 - p^2}} \approx -2p \int_p^\infty \frac{\nu' dy}{\sqrt{y^2 - p^2}}, \tag{5.4}$$

where $\nu = n - 1$ is refractivity. The representation of the forward model in the form of the Abel transform (5.4) allow the analytical solution of (5.3). Efficient numerical implementation of the forward modelling is discussed in PUBL.IV.

5.2 Inversion algorithm

Applying the inverse Abel transform, we can obtain the refractive index from the reconstruction formula

$$n(y) = \exp\left(\frac{1}{\pi} \int_y^\infty \frac{\alpha(p) dp}{\sqrt{p^2 - y^2}}\right), \tag{5.5}$$

where $y = n(r)r$ is the refractive altitude. Real geometric altitudes can be determined as

$$z = \frac{y}{n(y)} - R, \tag{5.6}$$

where R is the apparent Earth radius (the local radius of curvature of the Earth surface). The integration of equation (5.5) can be carried out numerically using any standard quadrature method. The weak singularity of the integrand at the lower limit does not cause problems for a numerical realization: the value of the integral at the vicinity of the singular point can be estimated or the midpoint product integration method can be applied [PUBL.IV].

The reconstruction of the refractive index from refractive angle measurements is a well-posed inverse problem [PUBL.IV]: the inversion operator (5.5) corresponds to fractional integration of order 1/2 and thus has a good smoothing effect on possible noise inherent in values $\alpha(p)$. Different discretization methods are discussed in PUBL.IV.

The density profile can then be obtained using Edlen's formula (5.1). By using the hydrostatic equation we can calculate the pressure P at the altitude z as

$$P(z) = \int_z^\infty g(x)\rho(x)dx, \tag{5.7}$$

where $g(x)$ is the acceleration of gravity. Finally, temperature can be determined from the equation of state of an ideal gas

$$T(z) = k\frac{P(z)}{\rho(z)}. \tag{5.8}$$

The influence of different error sources (instrumental noise, limited sampling frequency, scintillation, chromatic smoothing, forward modelling errors) on the retrieval performance is discussed in PUBL.V and in PUBL.VI.

5.3 A priori information in inverse problems from refractive measurements

Inclusion of a priori information in the form of the Bayesian optimal estimation can significantly improve the accuracy of the retrievals from radio occultation data [Rieder and Kirchengast, 2001]. A similar approach can be also applied to the inversion of stellar occultation measurements. The availability of relatively good a priori information – density and temperature data from ECMWF (European Centre for Medium-range Weather Forecast) – prompts the application of the Bayesian approach (MAP method). The inversion steps are linear (except for the last one: reconstruction of temperature from density and pressure); therefore, a priori information can be included either in retrieval of refractive angle or refractivity or density. The forward model can be written as

$$\mathbf{x}_{\text{meas}} = \mathbf{x} + \boldsymbol{\varepsilon}, \tag{5.9}$$

where $\mathbf{x}_{\text{meas}}$ presents a vector of measured parameters (refractive angle, refractivity or density), $\mathbf{x}$ is a vector of unknown parameters and $\boldsymbol{\varepsilon}$ is a vector of noise.

Provided that a priori profile $\mathbf{x}_{\text{prior}}$ and the measurement noise $\boldsymbol{\varepsilon}$ are Gaussian: $\mathbf{x}_{\text{prior}} \sim \mathcal{N}(\mathbf{x}_a, \mathbf{C}_a)$, $\boldsymbol{\varepsilon} \sim \mathcal{N}(0, \mathbf{C}_\varepsilon)$, the MAP estimate $\mathbf{x}_{\text{opt}}$ is the weighted combination of the a priori profile $\mathbf{x}_a$ and the reconstructed profile $\mathbf{x}_{\text{meas}}$

$$\mathbf{x}_{\text{opt}} = \mathbf{x}_a + \mathbf{C}_a(\mathbf{C}_\varepsilon + \mathbf{C}_a)^{-1}(\mathbf{x}_{\text{meas}} - \mathbf{x}_a). \tag{5.10}$$

The optimization affects the retrieval mainly in the upper atmosphere, where the signal-to-noise ratio is low, while in the lower atmosphere the retrieval is dominated by observation data. The prior covariance $\mathbf{C}_a$ can be taken, e.g., in the form

$$\mathbf{C}_a(i,j) = \sigma_i \sigma_j \exp\left(\frac{-|z_i - z_j|}{L}\right), \tag{5.11}$$

where z_i denotes an altitude grid point, σ_i is the standard deviation for the a priori profile at the point z_i and L is the characteristic scale defining the profile smoothness. Alternatively, a Gaussian or a triangular shape of the correlation function can be used.

The inclusion of a priori information in the density profile retrieval is discussed in Publ.VI. It is shown that the inclusion of a priori information significantly improves the accuracy of reconstruction, but the vertical resolution is degraded at high altitudes.

The GOMOS refractive angles can be retrieved from the pointing data of the Steering Front Assembly (SFA) and the star tracker (SATU). The sampling frequencies of SFA and SATU recordings are 10 Hz and 100 Hz, respectively. This gives resolution better than 300 m in the lower atmosphere. At the moment, the GOMOS pointing data are in the validation phase.

6 Summaries of original publications

I V. F. Sofieva, J. Tamminen, H. Haario, E. Kyrölä and M. Lehtinen: Ozone profile smoothness as a priori information in the inversion of limb measurements, *Annales Geophysicae*, 2004, Vol. 22, No. 10, pp. 3411–3420

Publ.I discusses inclusion of a priori information about smoothness of atmospheric profiles in inversion algorithms. Two recently proposed retrieval methods are further developed. One of them – Tikhonov-type regularization according to the target resolution – develops the classical Tikhonov regularization. The second method includes a priori information about the smoothness of atmospheric profiles in the form of Bayesian optimal estimation. A grid-independent formulation for the proposed inversion methods is proposed, thus isolating the choice of calculation grid from the question of how strong the smoothing should be. The approaches discussed are applied to the problem of ozone profile retrieval from stellar occultation measurements by the GOMOS instrument on board the Envisat satellite. Realistic simulations for the typical measurement conditions with smoothness a priori information created from 10-years analysis of ozone sounding at Sodankylä and analysis of total retrieval error illustrate the advantages of the proposed methods. The proposed methods are equally applicable to other profile retrieval problems from remote sensing measurements.

II V. F. Sofieva, E. Kyrö, E. Kyrölä: Smoothness of ozone profiles: analysis of 11-years of ozone sonde measurements at Sodankylä, *Annales Geophysicae*, 2004, Vol.22, No.8, pp. 2723-2727

In Publ.II, the methodology for creating a priori information about smoothness of atmospheric profiles is developed. This information can be used in advanced inversion methods for remote sensing measurements (considered in Publ.I) and in the instrument design for defining the vertical resolution requirements. The smoothness of the ozone profile is characterized by the characteristic scale of the fine structure, which, in turn, is defined as the correlation length of the ozone profile fluctuations. The analysis of the smoothness of ozone profiles based on 11-years ozone sonde measurements at Sodankylä is performed. It is found that the characteristic scale has only slight seasonal variations and can therefore be considered as a relatively stable atmospheric characteristic. The mean values of the characteristic scale are $\sim$ 1 km for altitudes below 10 km, and $\sim$ 1.4 km for altitudes 10–25 km.

III V. F. Sofieva and E. Kyrölä: Information approach to optimal selection of the spectral channels, *Journal of Geophysical Research*, 108(D16) 4513, doi: 10.1029/2002JD002980, 2003

In PUBL.III, methods for the selection of measurement subsets using information theory are examined. These methods are applied to an overdetermined inverse problem typical to high-resolution spectrometry. Two optimization problems in channel selection, both taking the information content of the measurements as a criterion, are defined and discussed. The concept of the information content of each individual measurement is introduced, and basic analytical relations are derived. A sequential deselecting procedure is developed and a fast algorithm for channel selection is proposed. These provide approximations to solutions of the optimization problem. The efficiencies of these selection procedures and a sequential selection procedure [*Rodgers*, 1996] are compared by means of a Monte Carlo generation of the forward model in a low-dimensional case. As a real application, the selection of the most informative spectral channels in UV-Visible wavelength range for GOMOS measurements is considered.

IV V. F. Sofieva and E. Kyrölä: Abel integral inversion in occultation measurements, in *Occultations for Probing Atmosphere and Climate*, edited by G. Kirchengast, U. Foelshe and A. Steiner, Springer Verlag, 2004, pp. 77- 86

In PUBL.IV, it is shown that occultation geometry under a spherical symmetry assumption leads to models described by the Abel integral equations. Analyzing general properties of the Abel transform, this work derives practical rules for discretization and for solution of the inverse problems, containing Abel-type integral equations. Two applications in remote sensing are considered: reconstruction of local densities from horizontal column densities (vertical inversion) in absorptive stellar occultation measurements and reconstruction of air density from refractive angle measurements. The ill- or well-posedness of these problems is discussed. Efficient discretization schemes are proposed, tested and compared with each other.

V V. F. Sofieva, E. Kyrölä, J. Tamminen and M. Ferraguto: Atmospheric density, pressure and temperature profile reconstruction from refractive angle measurements in stellar occultation, in *Occultations for Probing Atmosphere and Climate*, edited by G. Kirchengast, U. Foelshe and A. Steiner, Springer Verlag, 2004, pp. 289-298

In PUBL.V, the determination of the stratospheric density and temperature profiles from the refractive-angle measurements by stellar occultation instruments is considered. The forward model and the inversion algorithm are described. The error analysis was performed by Monte-Carlo simulations with additive Gaussian noise. The main error sources are identified and sensitivity of the inverse procedure to them is studied. The accuracy attainable in the temperature profiling with the present design of stellar occultation instruments is analyzed.

VI V. F. Sofieva, E. Kyrölä, M. Ferraguto and GOMOS CAL/VAL team: From pointing measurements in stellar occultation to atmospheric temperature, pressure and density profiling: simulations and first GOMOS results, IGARSS 2003, ISBN: 0-7803-7930-6 IEEE

PUBL.VI presents a feasibility study for retrieval of temperature and density profiles from pointing measurements by the GOMOS instrument. This study introduces extra geophysical parameters that can be obtained from the GOMOS instrument. Inclusion of a priori information is discussed and a realistic error analysis is carried out.

References

Backus, G. and Gilbert, F., Uniqueness in the inversion of inaccurate gross earth data, *Philos. Trans. Roy. Soc. London*, *Ser A*(266), 123–192, 1970.

Bennet, V. L., Dudhia, A., and Rodgers, C. D., Microwindows selection for MIPAS using information content, in *ESAMS99, European Symposium on Atmospheric Measurements from Space*, vol. WPP-161, pp. 265–270, ESA, Paris, 1999.

Bertaux, J. L., Hauchecorne, A., Dalaudier, F., Cot, C., Kyrölä, E., Fussen, D., Tamminen, J., Leppelmeier, G. W., Sofieva, V., Hassinen, S., d'Andon, O. F., Barrot, G., Mangin, A., Théodore, B., Guirlet, M., Korablev, O., Snoeij, P., Koopman, R., and Fraisse, R., First results on GOMOS/Envisat, *Adv. Space Res.*, *33*, 1029–1035, 2004.

Chu, W. P., McCormick, M. P., Lenoble, J., Brogniez, C., and Pruvost, P., SAGE-II inversion algorithm, *J. Geophys. Res.*, *94*, 8339–8351, 1989.

Dalaudier, F., Kan, V., and Gurvich, A. S., Chromatic refraction with global ozone monitoring by occultation of stars. I. Description and scintillation correction, *Applied Optics*, *40*(6), 866–877, 2001.

DeMajistre, R. and Yee, J.-H., Atmospheric remote sensing using a combined extinctive and refractive stellar occultation technique, 2. Inversion method for extinction measurements, *J. Geophys. Res.*, *107*(D15), doi:10.1029/2001JD000795, 2002.

Dudhia, A., Jay, V. L., and Rodgers, C. D., Microwindows selection for high-spectral-resolution sounders, *Applied Optics*, *41*, 3665–3673, 2002.

Edlen, B., The refractive index of air, *Metrologia*, *2*(71), 1966.

Elliot, J. L., Stellar occultation studies of the solar system, *Ann. Rev. Astron. Astrophys.*, *17*, 445–475, 1979.

Fortuin, J. P. F. and Kelder, H., An ozone climatology based on ozonesonde and satellite measurements, *J. Geophys. Res.*, *103*(D24), 31709–31734, 1998.

GOMOS ESL, *GOMOS Detailed Processing Model (DPM)*, ESA, 1998.

GOMOS ESL, *GOMOS Algorithm Theoretical Basis Document*, ESA, 1st edn., 1999.

Gorbunov, M. E. and Kornblueh, L., Analysis and validation of GPS/MET radio occultation data, *J. Geophys. Res.*, *106*(D15), 17161–17169, 2001.

Gorenflo, R. and Vessella, S., *Abel Integral Equations: Analysis and Applications.*, no. 1461 in Lecture Notes in Mathematics, Springer Verlag, 1991.

Gurvich, A. S. and Brekhovskikh, V., A study of turbulence and inner waves in the stratosphere based on the observations of stellar scintillations from space: A model of scintillation spectra, *Waves Random Media*, *11*, 163–181, 2001.

Gurvich, A. S. and Chunchuzov, I. P., Parameters of the fine density structure in the stratosphere obtained from spacecraft observations of stellar scintillation, *J. Geophys. Res.*, *108*, doi:10.1029/2002JD002281, 2003.

Haario, H., Laine, M., Lehtinen, M., Saksman, E., and Tamminen, J., MCMC methods for high dimensional inversion in remote sensing, *J. R. Statist. Soc. B*, *66*(Part 3), 591–607, 2004.

Hansen, P., Jacobsen, B. H., and Mosegaard, K., eds., *Methods and Applications of Inversion, Lecture Notes in Earth Science*, vol. 92, Springer, Berlin, 2000.

Hays, R. G. and Roble, P. B., Stellar spectra and atmospheric composition, *J. Atmos. Sci..*, *25*, 1141–1153, 1968.

Kaipio, J. and Somersalo, E., *Statistical and Computational Inverse Problems*, vol. 160 of *Applied Mathematical Sciences*, Springer, 2005.

Kan, V., Dalaudier, F., and Gurvich, A. S., Chromatic refraction with global ozone monitoring by occultation of stars. II. Statistical properties of scintillations, *Applied Optics*, *40*(6), 878–889, 2001.

Korpela, S., *A study of the operational principles of the GOMOS instrument for global ozone monitoring by the occultation of stars*, Geophysical publications, no. 22, Finnish Meteorological Institute, Helsinki, Ph.D thesis at the Helsinki University of Technology, 1991.

Kursinski, E. R., Hajj, G. A., Hardy, K. R., Schofield, J. T., and Linfield, R., Observing the Earth's Atmosphere with radio occultation measurements using the Global Position System, *J. Geophys. Res.*, *102*, 23429–23465, 1997.

Kyrölä, E., Sihvola, E., Kotivuori, Y., Tikka, M., Tuomi, T., and Haario, H., Inverse theory for occultation measurements, 1, Spectral inversion, *J. Geophys. Res.*, *98*, 7367–7381, 1993.

Kyrölä, E., Tamminen, J., Oikarinen, L., Sihvola, E., Verronen, P., and Leppelmeier, G. W., LIMBO—Limb and occultation measurement simulator, in *ESAMS99, European Symposium on Atmospheric Measurements from Space*, vol. WPP-161, pp. 487–493, ESA, Noordwijk, 1999.

Kyrölä, E., Tamminen, J., Leppelmeier, G. W., Sofieva, V., Hassinen, S., Bertaux, J.-L., Hauchecorne, A., Dalaudier, F., Cot, C., Korablev, O., d'Andon, O. F., Barrot, G., Mangin, A., Theodore, B., Guirlet, M., Etanchaud, F., Snoij, P.,

Koopman, R., Saavedra, L., Fraisse, R., Fussen, D., and Vanhellemont, F., GOMOS on Envisat: An overview, *Adv. Space Res.*, *33*, 1020–1028, 2004.

Kyrölä, E., Sofieva, V., Tamminen, J., Hauchecorne, A., Dalaudier, F., and GOMOS CAL/VAL team, Scintillation in stellar occultation: a nuisance for ozone monitoring or a source of information?, Proceedings of OPAC-2 International Workshop, submitted, 2005.

Lerner, J., Weisz, E., and Kirchengast, G., Temperature and humidity retrieval from simulated Infrared Atmospheric Sounding Interferometer (IASI) measurements, *J. Geophys. Res.*, *107*(D14), doi:10.1029/2001JD900254, 2002.

Morozov, V. A., *Regularization methods for ill-posed problems.*, CRC Press, Boca Raton, 1993.

Press, W. H., Teukolsky, S. A., Vetterling, W. T., and Flannery, B. P., *Numerical Recipes in FORTRAN, The Art of Scientific Computing*, Clarendon Press, Oxford, 1992.

Rieder, M. and Kirchengast, G., Error analysis and characterization of atmospheric profiles retrieved from GNSS occultation data, *J. Geophys. Res.*, *106*(D23), 31755–31770, 2001.

Roble, P. B. and Hays, R., A technique for recovering the vertical number density profile of atmospheric gases from planetary occultation data, *Planet Space Sci.*, *94*, 1727, 1972.

Rodgers, C. D., Characterization and error analysis of profiles retrieved from remote sounding measurements, *J. Geophys. Res.*, *95*(D5), 5587–5595, 1990.

Rodgers, C. D., Information content and optimization of high spectral resolution measurements, in *SPIE, Optical Spectroscopic techniques and Instrumentation for Atmospheric and Space Research II*, edited by P. B. Hay and J. Wang, vol. 2830, pp. 136–147, Int. Soc. for Opt. Eng., Bellingham, Wash., 1996.

Rodgers, C. D., *Inverse Methods for Atmospheric sounding: Theory and Practice*, World Scientific, Singapore, 2000.

Shannon, C. E. and Weaver, W., *The mathematical theory of communication*, Univ. of Ill. Press, Urbana, 1949.

Sihvola, E., *Coupling of spectral and vertical inversion in the analysis of stellar occultation data*, Geophysical publications, no. 38, Finnish Meteorological Institute, Helsinki, Licentiate thesis at the University of Helsinki, Department of Theoretical Physics, 1994.

Smith, G. E. and Hunten, D. M., Study of planetary atmospheres by absorptive occultations, *Reviews of Geophysics*, *28*, 117–143, 1990.

Sofieva, V. F., Tamminen, J., Kyrölä, E., and GOMOS CAL/VAL team, Modelling errors of GOMOS measurements: sensitivity study, Proceedings of OPAC-2 International Workshop, submitted, 2005.

Steiner, A., Kirchengast, G., and Landreiter, H. P., Inversion, error analysis and validation of GPS/MET occultation data, *Annales Geophysicae*, *17*, 122–138, 1999.

Tamminen, J., *Adaptive Markov chain Monte Carlo algorithms with Geophysical applications*, Finnish Meteorological Istitute Contributions, No. 47, Finnish Meteorological Institute, Helsinki, Finland, PhD thesis at the University of Helsinki, 2004.

Tamminen, J. and Kyrölä, E., Bayesian solution for nonlinear and non-Gaussian inverse problems by Markov chain Monte Carlo method, *J. Geophys. Res.*, *106*(D13), 14377–14390, 2001.

Tarantola, A., *Inverse Problem Theory, Methods for Data Fitting and Model Parameter Estimation*, Elsevier, New York, 1987.

Tatarskiy, V. I., Determining atmospheric density from satellite phase and refraction-angle measurements, *Izvestia Akad. Nauk, Atmospheric and Oceanic Physics*, *4*(7), 699–709, 1968.

Tatarskiy, V. I., The accuracy achievable in determining atmospheric density from satellite phase and refraction-angle measurements, *Izvestia Akad. Nauk, Atmospheric and Oceanic Physics*, *4*(8), 811–812, 1968.

Vanhellemont, F., Fussen, D., and Bingen, C., Global one-step inversion of satellite occultation measurements: A practical approach, *J. Geophys. Res.*, *109*(D09306), doi:10.1029/2003JD004168, 2004.

Vervack, R. J., Yee, J.-H., Carbary, J. F., and Morgan, F., Atmospheric remote sensing using a combined extinctive and refractive stellar occultation technique, 3. Inversion method for refraction measurements, *J. Geophys. Res.*, *107*(D15), doi:10.1029/2001JD000796, 2002.

Yee, J.-H., Jr., R. J. V., Demajistre, R., Morgan, F., Carbary, J. F., Romick, G. J., Morrison, D., Lloyd, S. A., DeCola, P. L., Paxton, L. J., Anderson, D. E., Kumar, C. K., and Meng, C.-I., Atmospheric remote sensing using a combined extinctive and refractive stellar occultation technique, 1. Overview and proof-of-concept observations, *J. Geophys. Res.*, *107*(D14), doi:10.1029/2001JD000794, 2002.